Hindawi
Mathematical Problems in Engineering
Volume 2017, Article ID 6271341, 16 pages
https://doi.org/10.1155/2017/6271341

Research Article

Neural Adaptive Decentralized Coordinated Control with Fault-Tolerant Capability for DFIGs under Stochastic Disturbances

Xiao-ming Li,[1] Xiu-yu Zhang,[1] Hong Cao,[2] Zhong-wei Lin,[3] Yu-guang Niu,[3] and Jian-guo Wang[1]

[1]*School of Automation Engineering, Northeast Electric Power University, Jilin 132012, China*
[2]*School of Economics and Management, Northeast Electric Power University, Jilin 132012, China*
[3]*State Key Laboratory of Alternate Electric Power System with Renewable Power Source, North China Electric Power University, Beijing 102206, China*

Correspondence should be addressed to Hong Cao; ch@ncepu.edu.cn

Received 9 March 2017; Accepted 25 July 2017; Published 10 October 2017

Academic Editor: Mohammad D. Aliyu

At present, most methodologies proposed to control over double fed induction generators (DFIGs) are based on single machine model, where the interactions from network have been neglected. Considering this, this paper proposes a decentralized coordinated control of DFIG based on the neural interaction measurement observer. An artificial neural network is employed to approximate the nonlinear model of DFIG, and the approximation error due to neural approximation has been considered. A robust stabilization technique is also proposed to override the effect of approximation error. A H_2 controller and a H_∞ controller are employed to achieve specified engineering purposes, respectively. Then, the controller design is formulated as a mixed H_2/H_∞ optimization with constrains of regional pole placement and proportional plus integral (PI) structure, which can be solved easily by using linear matrix inequality (LMI) technology. The results of simulations are presented and discussed, which show the capabilities of DFIG with the proposed control strategy to fault-tolerant control of the maximum power point tracking (MPPT) under slight sensor faults, low voltage ride-through (LVRT), and its contribution to power system transient stability support.

1. Introduction

During the last decade, wind power has shown world's fastest growing rate compared to any other electric power generations, which causes the share of wind power to reach a considerable level [1]. DFIG is becoming the dominant type used in wind farms (WFs) for its maximizing wind energy conversion and flexible control to network support [2]. For ensuring that DFIG is integrated into the power network reliably and efficiently, it is necessary to provide DFIGs with suitable control strategies.

Power system is a geographically extensive large-scale system, and its controller design is commonly based on decentralized approach which only depends on local signals [3–5]. However, this simple approach reduces the controller capability and even leads to stability problems [6]. Considering this, a few of decentralized coordinated control strategies of power system have been proposed [7–11]. A hierarchical decentralized coordinated control strategy is proposed to control the excitation system of synchronous generator (SG), where the interaction terms are considered as bounded disturbances which are suppressed by a H_∞ controller [8]. A direct feedback linearization based decentralized coordinated control of excitation and steam valve is proposed, where the upper bound of interaction terms is estimated [9]. A multiagent system based strategy is also used to control a multimachine power system [10, 11]. According methodologies used, decentralized coordinated control strategies of power system can be divided into two types, with and without communication system support. For the first type,

the interaction terms are commonly considered as bounded disturbances which are completely suppressed, where the involved coordinated information has been neglected, while the second method needs communication system support, which may bring new stability problems caused by communication time delay and communication system fault.

It is generally recognized that mode decomposition based decentralized coordinated control strategy is more suitable for control over power systems, where the interaction term is modelled as a coordinated signal [12, 13]. This allows the system-wide state feedback control strategy to be replaced by using local state feedback control, which is a desired performance for power system controller design. This paper proposes a neural observer based decentralized coordinated control of DFIG, where a neural controller is used to compute the weightings. The mode decomposition technology is used to modelling power system and a mixed H_2/H_∞ suboptimal control with regional pole placement and PI structure is employed to control a DFIG-based wind turbine. More concretely, the main contribution consists of the following aspects:

(i) The mode decomposition is used to modelling power system, and the interaction measurement model of DFIG is introduced (where interaction measurement term has been considered as a coordinated signal). An ANN-based weighting controller is proposed to approximate the nonlinear model of DFIG, which achieves a closed-loop nonlinear adaptive approximation.

(ii) The neural observer is proposed to approximate the nonlinear model of DFIG, where the approximation error due to the proposed neural approximation has been considered. A robust stabilization technique is proposed to override the effect of approximation error.

(iii) For improving the fault-tolerant capability, a H_∞ controller is employed to cope with the slight faults represented by bounded stochastic disturbances, and a H_2 controller with PI structure is also employed to achieve specified engineering purposes. Then, the controller design is formulated as a mixed H_2/H_∞ suboptimal problem with regional pole placement which is used to further improve damping performance.

(iv) The proposed control strategy combines the merits of conventional PI control, robust stabilization control, and mixed H_2/H_∞ optimization. Simulation results show that the proposed controller not only improves the MPPT control with fault-tolerant capability bus also enhances system damping and LVRT capability, which greatly improves power system transient stability.

The rest part of this paper is arranged as follows. The neural interaction measurement observer of DFIG is proposed in Section 2. In Section 3, the mixed H_2/H_∞ control with regional pole placement based on the obtained interaction measurement model is proposed. In Section 4, simulation results are presented and discussed, which demonstrate the capabilities of the proposed control strategy to enhance MPPT performance under external disturbances and its contribution on power system transient stability support. Finally, the conclusions are drawn in the Section 5.

2. Neural Adaptive Interaction Measurement Observer of DFIG

The proposed control strategy shown in Figure 1 is comprised of two parts, the neural interaction measurement observer of DFIG and the mixed H_2/H_∞ controller. The neural interaction measurement observer is established at chosen operating conditions by considering the interactions from network, and a neural weighting controller is proposed to compute the weightings according the approximation error. Based on the obtained observer, the H_∞ controller and H_2 controller are designed separately for specified engineering purposes. Then, the controller design is formulated as a mixed H_2/H_∞ suboptimal problem with the constrains of PI controller structure and regional pole placement, and it can be solved easily by using LMI technology.

2.1. DFIG Model with Stochastic Disturbances. For obtaining a good balance between the accuracy and simplification, the ith DFIG nonlinear model is chosen as a third-order model [15], where the stator dynamic has been neglected.

Dynamic equations:

$$\begin{aligned}
\frac{d\omega_{ri}}{dt} &= \frac{1}{2H_{\text{tot}i}}\left(T_{mi} - T_{ei}\right)\\
\frac{dE'_{qi}}{dt} &= -s\omega_{si}E'_{di} + \omega_{si}\frac{L_{mi}}{L_{rri}}v_{dri}\\
&\quad - \frac{1}{T'_{0i}}\left[E'_{qi} - \left(X_{si} - X'_{si}\right)i_{dsi}\right]\\
\frac{dE'_{di}}{dt} &= s\omega_{si}E'_{qi} - \omega_{si}\frac{L_{mi}}{L_{rri}}v_{qri}\\
&\quad - \frac{1}{T'_{0i}}\left[E'_{di} + \left(X_{si} - X'_{si}\right)i_{qsi}\right].
\end{aligned} \tag{1}$$

Output equations:

$$\begin{aligned}
P_{si} &= -E'_{di}i_{dsi} - E'_{qi}i_{qsi}\\
Q_{si} &= E'_{di}i_{qsi} - E'_{qi}i_{dsi},
\end{aligned} \tag{2}$$

where

$$\begin{aligned}
E'_{di} &= -R_{si}i_{dsi} + X'_{si}i_{qsi} + u_{dsi}\\
E'_{qi} &= -R_{si}i_{qsi} - X'_{si}i_{dsi} + u_{qsi}
\end{aligned}$$

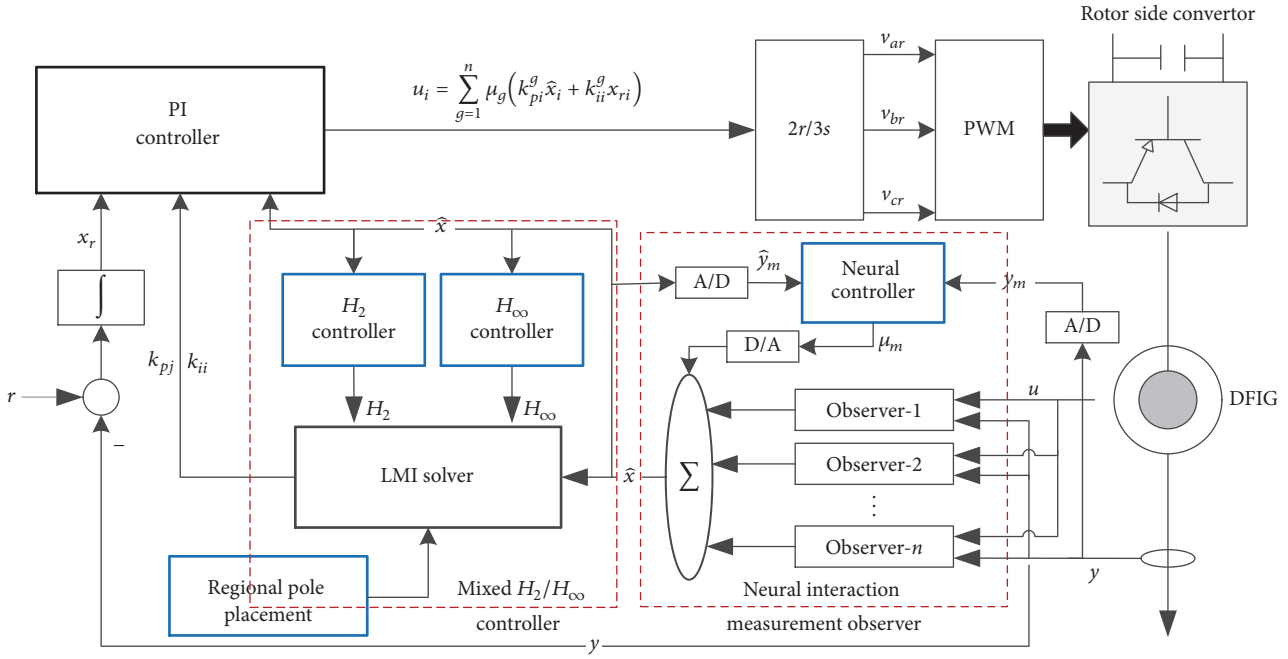

Figure 1: Neural PI control scheme.

$$i_{dsi} = -\left|E_i'\right| B_{ii} + \sum_{\substack{j=1 \\ j\neq i}}^{N} \left|E_j'\right| Y_{ij} \cos\left(\delta_{ij} - \alpha_{ij}\right)$$

$$i_{qsi} = \left|E_i'\right| G_{ii} + \sum_{\substack{j=1 \\ j\neq i}}^{N} \left|E_j'\right| Y_{ij} \sin\left(\delta_{ij} - \alpha_{ij}\right). \tag{3}$$

$X_{si}' = \omega_s(L_{ssi} - L_{mi}^2/L_{rri})$, $\delta_{ij} = \delta_i - \delta_j$, $\alpha_{ij} = 90 - \varphi_{ij}$, E_i' is the internal voltage of the ith generator, δ_i is the angle between the E_i' and the x-axis of the synchronous coordinates, φ_{ij} is the angle of impedance Z_{ij} ($Z_{ij} = (Y_{ij})^{-1}$), and N is the number of generators of a multimachine power system.

According the above equations, the ith DFIG nonlinear model with unmeasurable stochastic disturbances w_i and v_i can be written as the following compact form:

$$\begin{aligned} \dot{x}_i &= f_i(x_i) + g_i(x_i)\, u_i + d_{xi}\left(\left|E_j'\right|, \cos\left(\delta_{ij} - \alpha_{ij}\right)\right) \\ &\quad + w_i \\ y_i &= h_i(x_i) + d_{yi}\left(\left|E_j'\right|, \sin\left(\delta_{ij} - \alpha_{ij}\right)\right) + v_i, \end{aligned} \tag{4}$$

where $x_i = \left[\omega_{ri} \;\; E_{qi}' \;\; E_{di}'\right]^T$ is the state variable, $y_i = \left[P_{si} \;\; Q_{si}\right]^T$ is the output variable, $u_i = \left[u_{qri} \;\; u_{dri}\right]^T$ is the input signal (control vector), and $d_{xi}(|E_j'|, \cos(\delta_{ij} - \alpha_{ij}))$ and $d_{yi}(|E_j'|, \sin(\delta_{ij} - \alpha_{ij}))$ are the interaction terms from network.

2.2. Approximation Error Considered Interaction Measurement Observer. The published literatures [16, 17] extend the classical SG based interaction measurement modelling to DFIG field. The interaction measurement model of DFIG with a certain weighting method can be written as the following form, where the model bank is established at chosen operating points (Table 3) [16]:

$$\begin{aligned} \dot{x}_i &= \sum_{k=1}^{n} \mu_k \left(A_{ii}^k x_i + B_i^k u_i + T_{wi}^k + I_{mxi}^k\right) \\ y_i &= \sum_{k=1}^{n} \mu_k \left(C_{ii}^k x_i + I_{myi}^k\right), \end{aligned} \tag{5}$$

where $I_{mxi}^k = A_{2ii}^k \sum_{j=1,j\neq i}^{n} M_{ij} x_j = A_{2ii}^k(\Delta I_{si} - M_{ii} x_i)$ and $I_{myi}^k = C_{2ii}^k \sum_{j=1,j\neq i}^{n} M_{ij} x_j = C_{2ii}^k(\Delta I_{si} - M_{ii} x_i)$, M_{ij} denotes the interaction matrix from the ith node to the jth node, μ_k ($k = 1, \ldots, n$) is the weighting for the kth model in the model bank, and n is the number of model.

The terms I_{mxi}^k and I_{myi}^k are interaction measurement vectors, which represents interactions from network and can be regarded as coordinated signals. It is seen that I_{mxi}^k and I_{myi}^k only depend on local signals, which allows system-wide state feedback control to be replaced by using local state feedback method.

By combining (4)-(5), the approximation error considered interaction measurement model of DFIG can be rewritten as

$$\begin{aligned} \dot{x}_i &= \sum_{k=1}^{n} \mu_k \left(A_{ii}^k x_i + B_i^k u_i + T_{wi}^k + I_{mxi}^k\right) \\ &\quad + \left(f_i(x_i) - \sum_{k=1}^{n} \mu_k A_{ii}^k x_i\right) \end{aligned}$$

$$
\begin{aligned}
&+\left(g_i(x_i)-\sum_{k=1}^{n}\mu_k B_i^k\right)u_i\\
&+\left(d_{xi}\left(\left|E_j'\right|,\delta_{ij}\right)-\left(I_{mxi}^k+T_{wi}^k\right)\right)+w_i\\
&=\sum_{k=1}^{n}\mu_k\left(A_{ii}^k x_i+B_i^k u_i+T_{wi}^k+I_{mxi}^k\right)+\Delta f_i+\Delta g_i\\
&\quad+\Delta d_{xi}+w_i\\
y_i&=\sum_{k=1}^{n}\mu_k\left(C_{ii}^k x_i+I_{myi}^k\right)+\left(h_i(x_i)-\sum_{k=1}^{n}h_k C_{ii}^k x_i\right)\\
&\quad+\left(d_{yi}\left(\left|E_j'\right|,\delta_{ij}\right)-I_{myi}^k\right)+v_i\\
&=\sum_{k=1}^{n}\mu_k\left(C_{ii}^k x_i+I_{myi}^k\right)+\Delta h_i+\Delta d_{yi}+v_i,
\end{aligned}
\tag{6}
$$

where

$$\Delta f_i=f_i(x_i)-\sum_{k=1}^{n}\mu_k A_{ii}^k x_i \tag{7}$$

$$\Delta g_i=g_i(x_i)-\sum_{k=1}^{n}\mu_k B_i^k \tag{8}$$

$$\Delta h_i=h_i(x_i)-\sum_{k=1}^{n}\mu_k C_{ii}^k x_i \tag{9}$$

$$\Delta d_{xi}=d_{xi}\left(\left|E_j'\right|,\cos\left(\delta_{ij}-\alpha_{ij}\right)\right)-\sum_{k=1}^{n}\mu_k\left(I_{mxi}^k+T_{wi}^k\right) \tag{10}$$

$$\Delta d_{yi}=d_{yi}\left(\left|E_j'\right|,\sin\left(\delta_{ij}-\alpha_{ij}\right)\right)-\sum_{k=1}^{n}\mu_k I_{myi}^k. \tag{11}$$

In order to cope with the nonlinearity of DFIG, a neural observer is introduced to estimate the state variables of DFIG, where a neural controller is used to compute the weightings according the tracking error.

According (5) and (6), the observer can be written as

$$
\begin{aligned}
\dot{\widehat{x}}_i&=\sum_{k=1}^{n}\mu_k\left[A_{ii}^k\widehat{x}_i+B_i^k u_i+T_{wi}^k+I_{mxi}^k+L_i^k\left(y_i-\widehat{y}_i\right)\right]\\
&=\sum_{k=1}^{n}\mu_k\sum_{g=1}^{n}\mu_g\left[A_{ii}^k\widehat{x}_i+B_i^k u_i+T_{wi}^k+I_{mxi}^k+L_i^k C_{ii}^k e_i\right.\\
&\quad\left.+L_i^k\Delta h_i+L_i^k\Delta d_{yi}+L_i^k v_i\right],
\end{aligned}
\tag{12}
$$

where μ_k is the output of the ANN, $\widehat{y}_i=\sum_{k=1}^{n}\mu_k(C_{ii}^k\widehat{x}_i^k-I_{myi}^k)$ is the observer output, $e_i=x_i-\widehat{x}_i$ is the state estimation error, and

$$
\begin{aligned}
\dot{e}_i=\dot{x}_i-\dot{\widehat{x}}_i&=\sum_{k=1}^{n}\mu_k\sum_{g=1}^{n}\mu_g\left[\left(A_{ii}^k-L_i^k C_{ii}^g\right)e+\Delta f_i\right.\\
&\quad\left.+\Delta g_i+\Delta d_{xi}-L_i^k\Delta h_i-L_i^k\Delta d_{yi}-L_i^k v_i+w_i\right].
\end{aligned}
\tag{13}
$$

2.3. Neural Adaptive Weighting Controller. The Elman ANN can be described as the following equations [18]:

$$
\begin{aligned}
v_m&=W_m^U u_{\text{in}}+W_m^C X_m^C\\
X_m^H&=f_1(v_m)\\
X_m^C&=\alpha X_{m-1}^H\\
y_{\text{out}}&=f_2\left(W_m^O X_m^H\right),
\end{aligned}
\tag{14}
$$

where W_m^U, W_m^C, and W_m^O are weight matrixes of input layer, context unit, and output layer, respectively, u_{in} and y_{out} are the input and output vectors, respectively, v_m and X_m^H are the input and output vectors of hidden layer, respectively, X_m^C is the output vector of context unit, $f_1(\bullet)$ and $f_2(\bullet)$ are activation functions of hidden layer and output layer, and α is the self-feedback gain of context unit.

This paper employs an ANN controller shown in Figure 1 to approximate the nonlinear model of DFIG according the tracking error $x_{ei}(m)=y_i(m)-\widehat{y}_i(m)$, where m denotes the mth interval. The objective of the ANN controller is defined as

$$J_{Ni}(m)=\frac{1}{2}x_{ei}^T(m)\,Q_N x_{ei}(m)+\frac{1}{2}U_i^T(m)\,R_N U_i(m), \tag{15}$$

where $Q_N^T=Q_N>0$ and $R_N^T=R_N>0$ are weighting matrixes and $U_i(m)=\left[\mu_{i,1}^*(m)\ \cdots\ \mu_{i,n}^*(m)\right]$ is the output vector of the ANN (which is also the weightings represented by vector form).

The gradient descent method is employed to minimize the objective shown in (15). Then, the output layer weighting matrix of the ANN controller $W^O(m)$ can be updated as follows:

$$W^O(m)=W^O(m-1)-\eta\nabla_{W^O(m)}J_N(m), \tag{16}$$

where η is the learning rate and $\nabla_{W^O(m)}J_{Ni}(m)$ is the gradient of $J_{Ni}(m)$ with respect to $W^O(m)$.

$$
\begin{aligned}
\frac{\partial J_{Ni}(m)}{\partial W^O(m)}&=\frac{\partial J_{Ni}(m)}{\partial U_i(m)}\frac{\partial U_i(m)}{\partial W^O(m)}=\left\{-Q_N x_e(m)\right.\\
&\quad\left.\cdot\left[C^T(m)\,\widehat{x}_{i\cdot}(m)+\widetilde{I}_{myi}(m)\right]\right\}\frac{\partial U_i(m)}{\partial W^O(m)},
\end{aligned}
\tag{17}
$$

where $\widehat{y}_i(m)=\sum_{k=1}^{n}\mu_{i,k}(m)(C_{ii}^k(m)\widehat{x}_{i\cdot}(m)+I_{myi}^k(m))=U_i(m)(C^T(m)\widehat{x}_{i\cdot}(m)+\widetilde{I}_{myi}(m))$ is the observer output and $C^T(m)=\left[C_{ii}^1(m)\ \cdots\ C_{ii}^n(m)\right]^T$.

The term $\partial U_i(m)/\partial W^O(m)$ can be computed by the back-propagation method and no difficulty is involved in it. With a similar approach, the weighting matrixes of input layer and context unit can be updated. Then, the weighting vector U_i (which is also the output of the Elman ANN) can be updated adaptively according the mathematic model of the Elman ANN shown in (14). It is noted that, for obtaining the reasonable weightings, the activation function of the output layer is a sigmoid function $f(x)=1/(1+e^{-x})$, so that $0<\mu_k^*<1$.

By normalizing μ_k^*, the reasonable weightings can be obtained as $\mu_k = \mu_k^* / \sum_{g=1}^{n} \mu_g^*$ and $\sum_{k=1}^{n} \mu_k = 1$.

It can be seen that the weighting μ_k is regulated adaptively according the tracking error via a closed-loop approach. Considering the nonlinearity of ANN, the proposed weighting controller can be regarded as an adaptive nonlinear controller, which provides a desired approximation performance.

3. Controller Design

In this paper, the controller of rotor-side converter is chosen as the same structure as the conventional PI controller for taking its natural advantages of tracking control.

$$\begin{aligned} u_i &= \sum_{g=1}^{n} \mu_g \left(k_{pi}^g \hat{x}_i + k_{ii}^g \int_{t_0}^{t_f} r_i - \hat{y}_i dt \right) \\ &= \sum_{g=1}^{n} \mu_g \left(k_{pi}^g \hat{x}_i + k_{ii}^g x_{ri} \right), \end{aligned} \tag{18}$$

where k_{pi} and k_{ii} are the respective proportion coefficient and integration coefficient, r_i is the set point vector for the ith DFIG, $x_{ri} = \int_{t_0}^{t_f} (r_i - y_i) dt$ is the integral of tracking error, and

$$\begin{aligned} \dot{x}_{ri} &= r_i - y_i \\ &= r_i - \sum_{k=1}^{n} \mu_i^k \left[C_{ii}^k \left(\hat{x}_i + e_i \right) + I_{myi}^k \right] - \Delta h_i - \Delta d_{yi} \\ &\quad - v_i. \end{aligned} \tag{19}$$

By combining (12)–(19), the closed-loop system model can be written as

$$\begin{aligned} \begin{bmatrix} \dot{\hat{x}}_i \\ \dot{e}_i \\ \dot{x}_{ri} \end{bmatrix} &= \sum_{k=1}^{n} \mu_k \\ &\cdot \sum_{g=1}^{n} \mu_g \left(\begin{bmatrix} A_{ii}^k + B_{ii}^k k_{pi}^g & L_i^k C_{ii}^g & B_i^k k_{ii}^g \\ 0 & A_{ii}^k - {}^j L_i^k C_{ii}^g & 0 \\ C_{ii}^g & C_{ii}^g & 0 \end{bmatrix} \begin{bmatrix} \hat{x}_i \\ e_i \\ x_{ri} \end{bmatrix} \right. \\ &\left. + \begin{bmatrix} 0 & L_i^k \\ I & -L_i^k \\ 0 & -I \end{bmatrix} \begin{bmatrix} w_i \\ v_i \end{bmatrix} \right) + \begin{bmatrix} 0 \\ \Delta f_i \\ 0 \end{bmatrix} + \begin{bmatrix} 0 \\ \Delta g_i \\ 0 \end{bmatrix} \\ &+ \begin{bmatrix} \sum_{k=1}^{n} \mu_k L_i^k \Delta h_i \\ -\sum_{k=1}^{n} \mu_k L_i^k \Delta h_i \\ -\Delta h_i \end{bmatrix} + \begin{bmatrix} 0 \\ 0 \\ r_i \end{bmatrix} + \begin{bmatrix} \sum_{k=1}^{n} \mu_k I_{mxi}^k \\ 0 \\ -\sum_{k=1}^{n} \mu_k I_{myi}^k \end{bmatrix} \\ &+ \begin{bmatrix} 0 \\ \Delta d_{xi} \\ 0 \end{bmatrix} + \begin{bmatrix} \sum_{k=1}^{n} \mu_k L_i^k \Delta d_{yi} \\ -\sum_{k=1}^{n} \mu_k L_i^k \Delta d_{yi} \\ -\Delta d_{yi} \end{bmatrix} + \begin{bmatrix} \sum_{k=1}^{n} \mu_k T_{wi}^k \\ 0 \\ 0 \end{bmatrix}. \end{aligned} \tag{20}$$

By defining augment state vector $\overline{x}_i = \left[\hat{x}_i \;\; e_i \;\; x_{ri} \right]^T$, the compact form of (20) is

$$\begin{aligned} \dot{\overline{x}}_i &= \sum_{k=1}^{n} \mu_k \sum_{g=1}^{n} \mu_g \left(\overline{A}_i^{kg} \overline{x}_i + \overline{E}_i^k \overline{w}_i \right) + \Delta \overline{f}_i + \Delta \overline{g}_i + \Delta \overline{h}_{ii} \\ &\quad + \overline{I}_{mi} + \Delta \overline{d}_{xi} + \Delta \overline{d}_{yi} + \overline{T}_{wi} + \overline{r}_i, \end{aligned} \tag{21}$$

where

$$\overline{A}_i^{kg} = \begin{bmatrix} A_{ii}^k + B_{ii}^k k_{pi}^g & L_i^k C_{ii}^g & B_i^k k_{ii}^g \\ 0 & A_{ii}^k - {}^j L_i^k C_{ii}^g & 0 \\ C_{ii}^g & C_{ii}^g & 0 \end{bmatrix},$$

$$\overline{E}_i^k = \begin{bmatrix} 0 & L_i^k \\ I & -L_i^k \\ 0 & -I \end{bmatrix}$$

$$\Delta \overline{f}_i = \begin{bmatrix} 0 \\ \Delta f_i \\ 0 \end{bmatrix}$$

$$\Delta \overline{g}_i = \begin{bmatrix} 0 \\ \Delta g_i \\ 0 \end{bmatrix},$$

$$\overline{r} = \begin{bmatrix} 0 \\ 0 \\ r_i \end{bmatrix}_i$$

$$\Delta \overline{d}_{xi} = \begin{bmatrix} 0 \\ \Delta d_{xi} \\ 0 \end{bmatrix},$$

$$\Delta \overline{h}_{ii} = \begin{bmatrix} \sum_{k=1}^{n} \mu_k L_i^k \Delta h_i \\ -\sum_{k=1}^{n} \mu_k L_i^k \Delta h_i \\ -\Delta h_i \end{bmatrix},$$

$$\overline{I}_{mi} = \begin{bmatrix} \sum_{k=1}^{n} \mu_k I_{mxi}^k \\ 0 \\ -\sum_{k=1}^{n} \mu_k I_{myi}^k \end{bmatrix},$$

$$\Delta \overline{d}_{yi} = \begin{bmatrix} \sum_{k=1}^{n} \mu_k L_i^k \Delta d_{yi} \\ -\sum_{k=1}^{n} \mu_k L_i^k \Delta d_{yi} \\ -\Delta d_{yi} \end{bmatrix},$$

$$\overline{T}_{wi} = \begin{bmatrix} \sum_{k=1}^{n} \mu_k T_{wi}^k \\ 0 \\ 0 \end{bmatrix}. \tag{22}$$

Assumption 1. There exist bounding matrixes ΔA_i, ΔB_i, ΔC_i, ΔD_i, ΔE_i, ΔF_{xi}, and ΔF_{yi} such that

$$\|\Delta f_i\|_2 \le \|\Delta A_i x_i\|_2 \tag{23}$$

$$\|\Delta g_i\|_2 \le \left\| \sum_{k=1}^{n} \mu_k \Delta B_i \left(k_{pi}^k \widehat{x}_i + k_{ii}^k x_{ri} \right) \right\|_2 \tag{24}$$

$$\|\Delta h_i\|_2 \le \|\Delta C_i x_i\|_2 \tag{25}$$

$$\|\Delta d_{xi}\|_2 \le \|\Delta D_i x_i\|_2, \tag{26}$$

$$\|\Delta d_{yi}\|_2 \le \|\Delta E_i x_i\|_2, \tag{27}$$

$$\left\| \sum_{k=1}^{n} \mu_k I_{mxi}^k \right\|_2 \le \left\| \sum_{k=1}^{n} \mu_k \Delta F_{xi}^k x_i \right\|_2 \tag{28}$$

$$\left\| \sum_{k=1}^{n} \mu_k I_{myi}^k \right\|_2 \le \left\| \sum_{k=1}^{n} \mu_k \Delta F_{yi}^k x_i \right\|_2. \tag{29}$$

Since the parameters $\overline{T}_{wi}$ and $\overline{r}_i$ are limited by the capacity of a DFIG, their upper bounds can be easily determined as

$$\begin{aligned} \left\| \sum_{k=1}^{n} \mu_k T_{wi}^k \right\|_2 &\le \|\Delta H_i x_i\|_2 \\ \|r_i\|_2 &\le \|\Delta G_i x_i\|_2, \end{aligned} \tag{30}$$

where the details of ΔH_i and ΔG_i can be found in Appendix A.1.

According (23)–(30), we have

$$\begin{aligned} \left(\Delta\overline{f}_i\right)^T \left(\Delta\overline{f}_i\right) &= \left(\Delta f_i\right)^T \left(\Delta f_i\right) \le \left(\Delta A_i x_i\right)^T \left(\Delta A_i x_i\right) \\ &= \left(\left[\Delta A_i \;\; \Delta A_i \;\; 0\right]\overline{x}_i\right)^T \left(\left[\Delta A_i \;\; \Delta A_i \;\; 0\right]\overline{x}_i\right) \\ &= \left(\varphi_{fi}\overline{x}_i\right)^T \left(\varphi_{fi}\overline{x}_i\right) \end{aligned} \tag{31}$$

$$\begin{aligned} \left(\overline{r}_i\right)^T \left(\overline{r}_i\right) &\le \left(\Delta G_i x_i\right)^T \left(\Delta G_i x_i\right) = \left(\left[\Delta G_i \;\; \Delta G_i \;\; 0\right]\overline{x}_i\right)^T \\ &\cdot \left(\left[\Delta G_i \;\; \Delta G_i \;\; 0\right]\overline{x}_i\right) = \left(\varphi_{ri}\overline{x}_i\right)^T \left(\varphi_{ri}\overline{x}_i\right) \end{aligned} \tag{32}$$

$$\begin{aligned} \left(\Delta\overline{g}_i\right)^T \left(\Delta\overline{g}_i\right) &= \left(\Delta g_i\right)^T \left(\Delta g_i\right) \le \left(\sum_{k=1}^{n} \mu_k \left(\Delta B_i k_{pi}^k \widehat{x}_i \right. \right. \\ &\left. \left. + \Delta B_i {}^k k_{ii}^k x_{ri} \right) \right)^T \left(\sum_{k=1}^{n} \mu_k \left(\Delta B_i k_{pi}^k \widehat{x}_i + \Delta B_i {}^k k_{ii}^k x_{ri} \right) \right) \\ &= \left(\sum_{k=1}^{n} \mu_k \left[\Delta B_i k_{pi}^k \;\; 0 \;\; \Delta B_i k_{ii}^k \right] \overline{x}_i \right)^T \left(\sum_{k=1}^{n} \mu_k \right. \\ &\left. \cdot \left[\Delta B_i k_{pi}^k \;\; 0 \;\; \Delta B_i k_{ii}^k \right] \overline{x}_i \right) \le \sum_{k=1}^{n} \mu_k \left\{ \left({}^k\varphi_{gi}\overline{x}_i \right)^T \right. \\ &\left. \cdot \left({}^k\varphi_{gi}\overline{x}_i \right) \right\} \end{aligned} \tag{33}$$

$$\begin{aligned} \left(\Delta\overline{h}_i\right)^T \left(\Delta\overline{h}_i\right) &= 2 \left(\sum_{k=1}^{n} \mu_k L_i^k \Delta h_i \right)^T \left(\sum_{k=1}^{n} \mu_k L_i^k \Delta h_i \right) \\ &+ \Delta h_i^T \Delta h_i \le 2 \left(\sum_{k=1}^{n} \mu_k \Delta C_i x_i \right)^T \left(\sum_{k=1}^{n} \mu_k \Delta C_i x_i \right) \\ &+ \left(\Delta C_i x_i\right)^T \Delta C_i x_i = 2 \left(\sum_{k=1}^{n} \mu_k \right. \\ &\left. \cdot \left[L_i^k \Delta C_i \;\; L_i^k \Delta C_i \;\; 0 \right] x_i \right)^T \left(\sum_{k=1}^{n} \mu_k \right. \\ &\left. \cdot \left[L_i^k \Delta C_i \;\; L_i^k \Delta C_i \;\; 0 \right] x_i \right) + \left(\left[\Delta C_i \;\; \Delta C_i \;\; 0\right] \overline{x}_i \right)^T \\ &\cdot \left(\left[\Delta C_i \;\; \Delta C_i \;\; 0\right] \overline{x}_i \right) \le 2 \sum_{k=1}^{n} \mu_k \left\{ \left(\varphi_{h1i}^k \overline{x}_{ii} \right)^T \right. \\ &\left. \cdot \left(\varphi_{h1i}^k \overline{x}_{ii} \right) \right\} + \left(\varphi_{h2i} \overline{x}_i \right)^T \left(\varphi_{h2i} \overline{x}_i \right) \end{aligned} \tag{34}$$

$$\begin{aligned} \left(\Delta\overline{d}_{xi}\right)^T \left(\Delta\overline{d}_{xi}\right) &\le \left(\Delta D_i x_i\right)^T \left(\Delta D_i x_i\right) \\ &= \left(\left[\Delta D_i \;\; \Delta D_i \;\; 0\right]\overline{x}_i\right)^T \left(\left[\Delta D_i \;\; \Delta D_i \;\; 0\right]\overline{x}_i\right) \\ &= \left(\varphi_{dxi}\overline{X}_i\right)^T \left(\varphi_{dxi}\overline{X}_i\right) \end{aligned} \tag{35}$$

$$\begin{aligned} \left(\Delta\overline{d}_{yi}\right)^T \left(\Delta\overline{d}_{yi}\right) &= 2 \left(\sum_{k=1}^{n} \mu_k L_i^k \Delta d_{yi} \right)^T \left(\sum_{k=1}^{n} \mu_k \right. \\ &\left. \cdot L_i^k \Delta d_{yi} \right) + \left(\Delta d_{yi}\right)^T \left(\Delta d_{yi}\right) \le 2 \left(\sum_{k=1}^{n} \mu_k \Delta E_i x_i \right)^T \\ &\cdot \left(\sum_{k=1}^{n} \mu_k \Delta E_i x_i \right) + \left(\Delta E_i x_i\right)^T \Delta E_i x_i = 2 \left(\sum_{k=1}^{n} \mu_k \right. \\ &\left. \cdot \left[{}^j L_i \Delta E_i \;\; {}^j L_i \Delta E_i \;\; 0 \right] \overline{x}_i \right)^T \left(\sum_{k=1}^{n} \mu_k \right. \\ &\left. \cdot \left[{}^j L_i \Delta E_i \;\; {}^j L_i \Delta E_i \;\; 0 \right] \overline{x}_i \right) + \left(\left[\Delta E_i \;\; \Delta E_i \;\; 0\right] \overline{x}_i \right)^T \\ &\cdot \left(\left[\Delta E_i \;\; \Delta E_i \;\; 0\right] \overline{x}_i \right) \le 2 \sum_{k=1}^{n} \mu_k \left\{ \left(\varphi_{dy1i}^k \overline{x}_i \right)^T \right. \end{aligned}$$

$$\cdot \left(\varphi_{dy1i}^{k}\overline{x}_i\right)\Big\} + \left(\varphi_{dy2i}\overline{x}_i\right)^T\left(\varphi_{dy2i}\overline{x}_i\right) \tag{36}$$

$$\begin{aligned}\left(\overline{T}_{wi}\right)^T\left(\overline{T}_{wi}\right) &= \left(\sum_{k=1}^{n}\mu_k T_{wi}^k\right)^T\left(\sum_{k=1}^{n}\mu_k T_{wi}^k\right)\\ &\le \left(\Delta H_i x_i\right)^T\left(\Delta H_i x_i\right) = \left(\left[\Delta H_i \;\; \Delta H_i \;\; 0\right]\overline{x}_i\right)^T\\ &\cdot \left[\Delta H_i \;\; \Delta H_i \;\; 0\right]\overline{x}_i \le \left(\varphi_{di}\overline{x}_i\right)^T\left(\varphi_{di}\overline{x}_i\right)\end{aligned} \tag{37}$$

$$\begin{aligned}\left(\Delta\overline{I}_{mi}\right)^T\left(\Delta\overline{I}_{mi}\right) &= \left(\sum_{k=1}^{n}\mu_k I_{mxi}^k\right)^T\left(\sum_{k=1}^{n}\mu_k I_{mxi}^k\right)\\ &+ \left(\sum_{k=1}^{n}\mu_k I_{myi}^k\right)^T\left(\sum_{k=1}^{n}\mu_k I_{myi}^k\right) \le \left(\sum_{k=1}^{n}\mu_k \Delta F_{xi}^k x_i\right)^T\\ &\cdot \left(\sum_{k=1}^{n}\mu_k \Delta F_{xi}^k x_i\right) + \left(\sum_{k=1}^{n}\mu_k \Delta F_{yi}^k x_i\right)^T\\ &\cdot \left(\sum_{k=1}^{n}\mu_k \Delta F_{yi}^k x_i\right) = \left(\sum_{k=1}^{n}\mu_k\left[\Delta F_{xi}^k \;\; \Delta F_{xi}^k \;\; 0\right]\overline{x}_i\right)^T\\ &\cdot \left(\sum_{k=1}^{n}\mu_k\left[\Delta F_{xi}^k \;\; \Delta F_{xi}^k \;\; 0\right]\overline{x}_i\right)\\ &+ \left(\sum_{k=1}^{n}\mu_k\left[\Delta F_{yi}^k \;\; \Delta F_{yi}^k \;\; 0\right]\overline{x}_i\right)^T\\ &\cdot \left(\sum_{k=1}^{n}\mu_k\left[\Delta F_{yi}^k \;\; \Delta F_{yi}^k \;\; 0\right]\overline{x}_i\right)\\ &\le \sum_{k=1}^{n}\mu_k\left\{\left({}^j\varphi_{mxi}\overline{x}_i\right)^T\left({}^j\varphi_{mxi}\overline{x}_i\right)\right.\\ &\left.+ \left({}^j\varphi_{myi}\overline{x}_i\right)^T\left({}^j\varphi_{myi}\overline{x}_i\right)\right\},\end{aligned} \tag{38}$$

where $\varphi_{fi} = [\Delta A_i \;\; \Delta A_i \;\; 0]$, $\varphi_{gi}^k = \left[\Delta B_i k_{pi}^k \;\; 0 \;\; \Delta B_i k_{ii}^k\right]$, $\varphi_{h1i}^k = \left[L_i^k \Delta C_i \;\; L_i^k \Delta C_i \;\; 0\right]$, $\varphi_{h2i} = [\Delta C_i \;\; \Delta C_i \;\; 0]$, $\varphi_{ri} = [\Delta G_i \;\; \Delta G_i \;\; 0]$, $\varphi_{dxi} = [\Delta D_i \;\; \Delta D_i \;\; 0]$, $\varphi_{dy1i}^k = \left[L_i^k \Delta E_i \;\; L_i^k \Delta E_i \;\; 0\right]$, $\varphi_{dy2i} = [\Delta E_i \;\; \Delta E_i \;\; 0]$, $\varphi_{mxi}^k = \left[\Delta F_{xi}^k \;\; \Delta F_{xi}^k \;\; 0\right]$, $\varphi_{myi}^k = \left[\Delta F_{yi}^k \;\; \Delta F_{yi}^k \;\; 0\right]$, and $\varphi_{di} = [\Delta H_i \;\; \Delta H_i \;\; 0]$.

3.1. H_∞ Controller Design. The H_∞ control is the common solution for external disturbance rejection, of which objective can be defined as

$$\begin{aligned}J_\infty^i &= \int_{t_0}^{t_f}\overline{x}_i^T Q_{1i}\overline{x}\,dt\\ &\le \overline{x}_i^T\left(t_0\right)P_{1i}\overline{x}\left(t_0\right) + \rho^2\int_{t_0}^{t_f}\overline{w}_i^T\left(t\right)\overline{w}_i\left(t\right)dt,\end{aligned} \tag{39}$$

where ρ is a prescribed attenuation level and weighting matrixes ${P_{1i}}^T = P_{1i} > 0$ and ${Q_{1i}}^T = Q_{1i} > 0$.

A Lyapunov function for system of (21) is chosen as following form:

$$V\left(\overline{x}\right) = \overline{x}^T P\overline{x}. \tag{40}$$

By differentiating (40), we obtain

$$\begin{aligned}\dot{V} &= \dot{\overline{x}}_i^T P_{i1}\overline{x}_i + \overline{x}_i^T P_{i1}\dot{\overline{x}}\\ &= \left(\sum_{k=1}^{n}\mu_k\sum_{g=1}^{n}\mu_g\left(\overline{A}_i^{kg}\overline{x}_i + \overline{E}_i{}^k\overline{w}_i\right) + \Delta f_{gh}\right)^T P_{1i}\overline{x}_i\\ &\quad + \overline{x}_i^T P_{1i}\left(\sum_{k=1}^{n}\mu_k\sum_{g=1}^{n}\mu_g\left(\overline{A}_i^{kg}\overline{x}_i + \overline{E}_i{}^k\overline{w}_i\right) + \Delta f_{gh}\right)\\ &= \left(\sum_{k=1}^{n}\mu_k\sum_{g=1}^{n}\mu_g\overline{A}_i^{kg}\overline{x}_i\right)^T P_{1i}\overline{x}_i\\ &\quad + \overline{x}_i^T P_{1i}\left(\sum_{k=1}^{n}\mu_k\sum_{g=1}^{n}\mu_g\overline{A}_i^{kg}\overline{x}_i\right)\\ &\quad + \left(\sum_{k=1}^{n}\mu_k\overline{E}_i{}^k\overline{w}_i\right)^T P_{1i}\overline{x}_i + \overline{x}_i^T P_{1i}\left(\sum_{k=1}^{n}\mu_k\overline{E}_i{}^k\overline{w}_i\right)\\ &\quad + \Delta f_{gh}^T P_{1i}\overline{x}_i + \overline{x}_i^T P_{1i}\Delta f_{gh},\end{aligned} \tag{41}$$

where $\Delta f_{gh} = \Delta\overline{f}_i + \Delta\overline{g}_i + \Delta\overline{h}_i + \overline{r}_i + \overline{I}_{mi} + \Delta\overline{d}_{xi} + \Delta\overline{d}_{yi} + \overline{T}_{wi}$.

Lemma 2. *Give two vectors $x \in R^n$ and $y \in R^n$; the following inequality is identical:*

$$\begin{aligned}&x^T y + y^T x - \xi^2 x^T x - \xi^{-2} y^T y\\ &\quad = -\left(\xi x^T - \xi^{-1} y\right)^T\left(\xi x^T - \xi^{-1} y\right) \le 0 \quad (\xi \ne 0).\end{aligned} \tag{42}$$

According Lemma 2, the following inequalities can be obtained:

$$\begin{aligned}&\left(\sum_{k=1}^{n}\mu_k\overline{E}_i{}^k\overline{w}_i\right)^T P_{1i}\overline{x}_i + \overline{x}_i^T P_{1i}\left(\sum_{k=1}^{n}\mu_k\overline{E}_i{}^k\overline{w}_i\right)\\ &\quad \le \rho^{-2}\overline{x}_i^T P_{1i}\left(\sum_{k=1}^{n}\mu_k\overline{E}_i{}^k\right)\left(\sum_{k=1}^{n}\mu_k\overline{E}_i{}^k\right)^T P_{1i}\overline{x}_i\\ &\quad + \rho^2\overline{w}_i^T\overline{w}_i\end{aligned} \tag{43}$$

$$\begin{aligned}\Delta f_{gh}^T P_{1i}\overline{x}_i + \overline{x}_i^T P_{1i}\Delta f_{gh} &= \left(\Delta\overline{f}_i + \Delta\overline{g}_i + \Delta\overline{h}_i + \overline{r}_i\right.\\ &\quad \left.+ \overline{I}_{mi} + \Delta\overline{d}_{xi} + \Delta\overline{d}_{yi} + \overline{T}_{wi}\right)^T P_{1i}\overline{x}_i + \overline{x}_i^T P_{1i}\left(\Delta\overline{f}_i\right.\\ &\quad \left.+ \Delta\overline{g}_i + \Delta\overline{h}_i + \overline{r}_i + \overline{I}_{mi} + \Delta\overline{d}_{xi} + \Delta\overline{d}_{yi} + \overline{T}_{wi}\right)\\ &\le 8\overline{x}_i^T P_{1i}P_{1i}\overline{x}_i + \left(\Delta\overline{f}_i\right)^T\left(\Delta\overline{f}_i\right) + \left(\Delta\overline{g}_i\right)^T\left(\Delta\overline{g}_i\right)\\ &\quad + \left(\Delta\overline{h}_i\right)^T\left(\Delta\overline{h}_i\right) + \left(\overline{r}_i\right)^T\left(\overline{r}_i\right) + \left(\overline{I}_{mi}\right)^T\left(\overline{I}_{mi}\right)\\ &\quad + \left(\Delta\overline{d}_{xi}\right)^T\left(\Delta\overline{d}_{xi}\right) + \left(\Delta\overline{d}_{yi}\right)^T\left(\Delta\overline{d}_{yi}\right) + \left(\overline{T}_{wi}\right)^T\\ &\quad \cdot\left(\overline{T}_{wi}\right).\end{aligned} \tag{44}$$

By using (31)–(37), (44) can be rewritten as

$$\begin{aligned}\Delta f_{gh}^T P_{1i}\overline{x}_i + \overline{x}_i^T P_{1i}\Delta f_{gh} &\le \left(\varphi_{fi}\overline{x}_i\right)^T\left(\varphi_{fi}\overline{x}_i\right) + \sum_{k=1}^{n}\mu_k\\ &\quad \cdot\left\{\left(\varphi_{gi}^k\overline{x}_i\right)^T\left(\varphi_{gi}^k\overline{x}_i\right)\right\} + 2\sum_{k=1}^{n}\mu_k\\ &\quad \cdot\left\{\left(\varphi_{h1i}^k\overline{x}_{ii}\right)^T\left(\varphi_{h1i}^k\overline{x}_{ii}\right)\right\} + \left(\varphi_{h2i}\overline{x}_i\right)^T\left(\varphi_{h2i}\overline{x}_i\right)\\ &\quad + \left(\varphi_{ri}\overline{x}_i\right)^T\left(\varphi_{ri}\overline{x}_i\right) + \left(\varphi_{dxi}\overline{x}_i\right)^T\left(\varphi_{dxi}\overline{x}_i\right) + 2\sum_{k=1}^{n}\mu_k\\ &\quad \cdot\left\{\left(\varphi_{dy1i}^k\overline{x}_i\right)^T\left(\varphi_{dy1i}^k\overline{x}_i\right)\right\} + \left(\varphi_{dy2i}\overline{x}_i\right)^T\left(\varphi_{dy2i}\overline{x}_i\right)\\ &\quad + \left(\varphi_{di}\overline{x}_i\right)^T\left(\varphi_{di}\overline{x}_i\right) + \sum_{k=1}^{n}\mu_k\\ &\quad \cdot\left\{\left(\varphi_{mxi}^k\overline{x}_i\right)^T\left(\varphi_{mxi}^k\overline{x}_i\right) + \left(\varphi_{myi}^k\overline{x}_i\right)^T\left(\varphi_{myi}^k\overline{x}_i\right)\right\}\\ &\quad + 8\overline{x}_i^T P_{1i}P_{1i}\overline{x}_i.\end{aligned} \tag{45}$$

According (43) and (45), (41) can be rewritten as

$$\begin{aligned}\dot{V} = \dot{\overline{x}}_i^T P_{i1}\overline{x}_i + \overline{x}_i^T P_{i1}\dot{\overline{x}} &\le \sum_{k=1}^{n}\mu_k\sum_{g=1}^{n}\mu_g\overline{x}_i^T\left\{\left(\overline{A}_i^{kg}\right)^T P_{1i}\right.\\ &\quad \left.+ P_{1i}\overline{A}_i^{kg} + \rho^{-2}P_{1i}\left(\overline{E}_i^{\,k}\left(\overline{E}_i^{\,k}\right)^T + 8I\right)P_{1i}\right.\\ &\quad \left.+ \left(\varphi_{fi}\right)^T\left(\varphi_{fi}\right) + \left(\varphi_{gi}^k\right)^T\left(\varphi_{gi}^k\right) + 2\left(\varphi_{h1i}^k\right)^T\left(\varphi_{h1i}^k\right)\right.\\ &\quad \left.+ \left(\varphi_{h2i}\right)^T\left(\varphi_{h2i}\right) + \left(\varphi_{ri}\right)^T\left(\varphi_{ri}\right) + \left(\varphi_{dxi}\right)^T\left(\varphi_{dxi}\right)\right.\\ &\quad \left.+ 2\left(\varphi_{dy1i}^k\right)^T\left(\varphi_{dy1i}^k\right) + \left(\varphi_{dy2i}\right)^T\left(\varphi_{dy2i}\right)\right.\\ &\quad \left.+ \left(\varphi_{di}\right)^T\left(\varphi_{di}\right) + \left(\varphi_{mxi}^k\right)^T\left(\varphi_{mxi}^k\right)\right.\\ &\quad \left.+ \left(\varphi_{myi}^k\right)^T\left(\varphi_{myi}^k\right)\right\}\overline{x}_i + \rho^2\overline{w}_i^T\overline{w}_i.\end{aligned} \tag{46}$$

Then, the following result can be obtained.

Theorem 3. *In the nonlinear augmented system (21), if $P_{1i}^T = P_{1i} > 0$ is the common solution for the matrix inequality*

$$\begin{aligned}&\left(\overline{A}_i^{kg}\right)^T P_{1i} + P_{1i}\overline{A}_i^{kg} + \rho^{-2}P_{1i}\left(\overline{E}_i^{\,k}\left(\overline{E}_i^{\,k}\right)^T + 8I\right)P_{1i}\\ &\quad + \left(\varphi_{fi}\right)^T\left(\varphi_{fi}\right) + \left(\varphi_{gi}^k\right)^T\left(\varphi_{gi}^k\right) + 2\left(\varphi_{h1i}^k\right)^T\left(\varphi_{h1i}^k\right)\\ &\quad + \left(\varphi_{h2i}\right)^T\left(\varphi_{h2i}\right) + \left(\varphi_{ri}\right)^T\left(\varphi_{ri}\right) + \left(\varphi_{dxi}\right)^T\left(\varphi_{dxi}\right)\\ &\quad + 2\left(\varphi_{dy1i}^k\right)^T\left(\varphi_{dy1i}^k\right) + \left(\varphi_{dy2i}\right)^T\left(\varphi_{dy2i}\right)\\ &\quad + \left(\varphi_{di}\right)^T\left(\varphi_{di}\right) + \left(\varphi_{mxi}^k\right)^T\left(\varphi_{mxi}^k\right)\\ &\quad + \left(\varphi_{myi}^k\right)^T\left(\varphi_{myi}^k\right) + Q_{1i} < 0\end{aligned} \tag{47}$$

for $k, g = 1, 2, \ldots, n$, then the performance of the proposed H_∞ controller shown in (39) is guaranteed for a prescribed ρ^2.

Proof. From (47),

$$\begin{aligned}&\left(\overline{A}_i^{kg}\right)^T P_{1i} + P_{1i}\overline{A}_i^{kg} + \rho^{-2}P_{1i}\left(\overline{E}_i^{\,k}\left(\overline{E}_i^{\,k}\right)^T + 8I\right)P_{1i}\\ &\quad + \left(\varphi_{fi}\right)^T\left(\varphi_{fi}\right) + \left(\varphi_{gi}^k\right)^T\left(\varphi_{gi}^k\right)\\ &\quad + 2\left(\varphi_{h1i}^k\right)^T\left(\varphi_{h1i}^k\right) + \left(\varphi_{h2i}\right)^T\left(\varphi_{h2i}\right) + \left(\varphi_{ri}\right)^T\left(\varphi_{ri}\right)\\ &\quad + \left(\varphi_{dxi}\right)^T\left(\varphi_{dxi}\right) + 2\left(\varphi_{dy1i}^k\right)^T\left(\varphi_{dy1i}^k\right)\\ &\quad + \left(\varphi_{dy2i}\right)^T\left(\varphi_{dy2i}\right) + \left(\varphi_{di}\right)^T\left(\varphi_{di}\right)\\ &\quad + \left(\varphi_{mxi}^k\right)^T\left(\varphi_{mxi}^k\right) + \left(\varphi_{myi}^k\right)^T\left(\varphi_{myi}^k\right) < -Q_{1i}.\end{aligned} \tag{48}$$

From (46) and (48), we get

$$\begin{aligned}\dot{V} = \dot{\overline{x}}_i^T P_{i1}\overline{x}_i + \overline{x}_i^T P_{i1}\dot{\overline{x}} &\le \sum_{k=1}^{n}\mu_k\sum_{g=1}^{n}\mu_g\overline{x}_i^T\left(-Q_{1i}\right)\overline{x}_i + \rho^2\overline{w}_i^T\overline{w}_i\\ &\le \overline{x}_i^T\left(-Q_{1i}\right)\overline{x}_i + \rho^2\overline{w}_i^T\overline{w}_i.\end{aligned} \tag{49}$$

By integrating (49) from $t = t_0$ to $t = t_f$, we have

$$V\left(t_f\right) - V\left(t_0\right) \le -\int_{t_0}^{t_f}\overline{x}_i^T Q_{1i}\overline{x}\,dt + \rho^2\int_{t_0}^{t_f}\overline{w}_i^T\overline{w}_i dt. \tag{50}$$

Then,

$$\begin{aligned}\int_{t_0}^{t_f}\overline{x}_i^T Q_{1i}\overline{x}\,dt &\le V\left(t_0\right) - V\left(t_f\right) + \rho^2\int_{t_0}^{t_f}\overline{w}_i^T\overline{w}_i dt\\ &\le \overline{x}_i^T P_{1i}\overline{x}_i + \rho^2\int_{t_0}^{t_f}\overline{w}_i^T\overline{w}_i dt.\end{aligned} \tag{51}$$

From (51), it is seen that, under the constrain of (47), the H_∞ control performance is achieved with a prescribed ρ^2. □

3.2. H_2 Controller Design. The H_2 controller (power regulator and automatic voltage regulator (AVR)) is developed, of which objective can be written as

$$\begin{aligned}&\min J_2^i(u_i)\\&= \int_{t_0}^{t_f}\left[(r_i-\widehat{y}_i)^T\widetilde{Q}_{2i}(r_i-\widehat{y}_i)+u_i^T R_i u_i\right]dt.\end{aligned}\tag{52}$$

Since that the external disturbances $\overline{w}_i$ have been efficiently eliminated by the proposed H_∞ controller, the H_2 controller should be designed without considering $\overline{w}_i$. For the approximation errors have been considered, it is hard to obtain the optimal solution of (52). Thus, a suboptimal method is employed to minimize its upper bound.

By substituting (18) into (52), we have

$$\begin{aligned}J_2^i(u_i) &= \int_{t_0}^{t_f}\Bigg[(r_i-\widehat{y}_i)^T\widetilde{Q}_{2i}(r_i-\widehat{y}_i)\\&\quad+\left(\sum_{g=1}^{n}\mu_g\left(k_{pi}^g\widehat{x}_i+k_{ii}^g x_{ri}\right)\right)^T\\&\quad\cdot R_i\left(\sum_{g=1}^{n}\mu_g\left(k_{pi}^g\widehat{x}_i+k_{ii}^g x_{ri}\right)\right)\Bigg]dt\\&\le\int_{t_0}^{t_f}\Bigg[(x_{ri})^T\widetilde{Q}_{2i}(x_{ri})+\left(\sum_{g=1}^{n}\mu_g\overline{K}_i^g\overline{x}_i\right)^T\\&\quad\cdot R_i\left(\sum_{g=1}^{n}\mu_g\overline{K}_i^g\overline{x}_i\right)+\frac{dt}{d}\left(\overline{x}_i^T P_{2i}\overline{x}_i\right)\Bigg]dt\\&\quad+\overline{x}_i^T(t_0)P_{2i}\overline{x}_i(t_0)-\overline{x}_i^T(t_f)P_{2i}\overline{x}_i(t_f)\\&\le\int_{t_0}^{t_f}\Bigg[(x_{ri})^T\widetilde{Q}_{2i}(x_{ri})+\left(\sum_{g=1}^{n}\mu_g\overline{K}_i^g\overline{x}_i\right)^T\\&\quad\cdot R_i\left(\sum_{g=1}^{n}\mu_g\overline{K}_i^g\overline{x}_i\right)+\dot{\overline{x}}_i^T P_{2i}\overline{x}_i+\overline{x}_i^T P_{2i}\dot{\overline{x}}_i\Bigg]dt\\&\quad+\overline{x}_i^T(t_0)P_{2i}\overline{x}_i(t_0),\end{aligned}\tag{53}$$

where $\overline{K}_i^g=\left[k_{pi}^k\ \ 0\ \ k_{ii}^k\right]$.

From (41) and (45), (53) can be rewritten as

$$\begin{aligned}J_2^i(u_i)\le&\int_{t_0}^{t_f}\Bigg((\overline{x}_i)^T Q_{2i}(\overline{x}_i)+\left(\sum_{g=1}^{n}\mu_g\overline{K}_i^g\overline{x}_i\right)^T\\&\cdot R_i\left(\sum_{g=1}^{n}\mu_g\overline{K}_i^g\overline{x}_i\right)\\&+\left(\sum_{k=1}^{n}\mu_k\sum_{g=1}^{n}\mu_g\overline{A}_i^{kg}\overline{x}_i\right)^T P_{1i}\overline{x}_i\\&+\overline{x}_i^T P_{1i}\left(\sum_{k=1}^{n}\mu_k\sum_{g=1}^{n}\mu_g\overline{A}_i^{kg}\overline{x}_i\right)\\&+\Delta f_{gh}^T P_{1i}\overline{x}_i+\overline{x}_i^T P_{1i}\Delta f_{gh}\Bigg)dt\\&+\overline{x}_i^T(t_0)P_{2i}\overline{x}_i(t_0)\\\le&\int_{t_0}^{t_f}\sum_{k=1}^{n}\mu_k\sum_{g=1}^{n}\mu_g(\overline{x}_i)^T\{Q_{2i}\\&+\left(\overline{K}_i^g\right)^T R_i\left(\overline{K}_i^g\right)\\&+\left(\overline{A}_i^{kg}\right)^T P_{1i}+P_{1i}\overline{A}_i^{kg}+\left(\varphi_{fi}\right)^T\left(\varphi_{fi}\right)\\&+\left(\varphi_{gi}^k\right)^T\left(\varphi_{gi}^k\right)+2\left(\varphi_{h1i}^k\right)^T\left(\varphi_{h1i}^k\right)\\&+\left(\varphi_{h2i}\right)^T\left(\varphi_{h2i}\right)+\left(\varphi_{ri}\right)^T\left(\varphi_{ri}\right)\\&+\left(\varphi_{dxi}\right)^T\left(\varphi_{dxi}\right)+2\left(\varphi_{dy1i}^k\right)^T\left(\varphi_{dy1i}^k\right)\\&+\left(\varphi_{dy2i}\right)^T\left(\varphi_{dy2i}\right)+\left(\varphi_{di}\right)^T\left(\varphi_{di}\right)\\&+\left(\varphi_{mxi}^k\right)^T\left(\varphi_{mxi}^k\right)+\left(\varphi_{myi}^k\right)^T\left(\varphi_{myi}^k\right)\Big\}\\&\cdot\overline{x}_i dt+\overline{x}_i^T(t_0)P_{2i}\overline{x}_i(t_0),\end{aligned}\tag{54}$$

if

$$\begin{aligned}&Q_{2i}+\left(\overline{K}_i^g\right)^T R_i\left(\overline{K}_i^g\right)+\left(\overline{A}_i^{kg}\right)^T P_{1i}+P_{1i}\overline{A}_i^{kg}\\&\quad+\left(\varphi_{fi}\right)^T\left(\varphi_{fi}\right)+\left(\varphi_{gi}^k\right)^T\left(\varphi_{gi}^k\right)+2\left(\varphi_{h1i}^k\right)^T\left(\varphi_{h1i}^k\right)\\&\quad+\left(\varphi_{h2i}\right)^T\left(\varphi_{h2i}\right)+\left(\varphi_{ri}\right)^T\left(\varphi_{ri}\right)+\left(\varphi_{dxi}\right)^T\left(\varphi_{dxi}\right)\\&\quad+2\left(\varphi_{dy1i}^k\right)^T\left(\varphi_{dy1i}^k\right)+\left(\varphi_{dy2i}\right)^T\left(\varphi_{dy2i}\right)\\&\quad+\left(\varphi_{di}\right)^T\left(\varphi_{di}\right)+\left(\varphi_{mxi}^k\right)^T\left(\varphi_{mxi}^k\right)\\&\quad+\left(\varphi_{myi}^k\right)^T\left(\varphi_{myi}^k\right)<0.\end{aligned}\tag{55}$$

From (55), the upper bound of the H_2 objective is obtained as

$$\begin{aligned}J_2^i(u_i)&\le\int_{t_0}^{t_f}\overline{x}_i^T(-Q_{2i})\overline{x}_i dt+\overline{x}_i^T(t_0)P_{2i}\overline{x}_i(t_0)\\&\le\overline{x}_i^T(t_0)P_{2i}\overline{x}_i(t_0)\end{aligned}\tag{56}$$

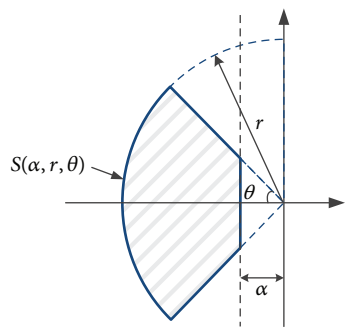

Figure 2: Region $S(\alpha, r, \theta)$.

Therefore, the suboptimal H_2 control can be formulated as following minimization problem:

$$\min_{P_{2i}} \quad \overline{x}_i^T(t_0) P_{2i} \overline{x}_i(t_0) \qquad \text{Subject to} \quad P_{2i} > 0 \text{ and } (55). \tag{57}$$

3.3. Mixed H_2/H_∞ Control with Regional Pole Placement. Since the H_∞ and H_2 controllers have been developed separately, the mixed H_2/H_∞ control is developed to satisfy both suboptimal H_2 performance in (56) and H_∞ performance in (39). The proposed mixed H_2/H_∞ controller can be formulated as the following suboptimization problem:

$$\min_{P_i} \quad \overline{x}_i^T(t_0) P_i \overline{x}_i(t_0) \tag{58}$$

$$\text{Subject to} \quad P_i = P_{1i} = P_{2i} > 0, \quad (47) \text{ and } (55). \tag{59}$$

In order to further improve DFIG damping performance, the poles of closed-loop system of (21) are placed within the region $S(\alpha, r, \theta)$ shown in Figure 2, of which characteristic LMI can be written as following forms [19]:

$$\begin{aligned} &\overline{A}_i^{kg} P_i + P_i^{jk} \left(\overline{A}_i^{kg}\right)^T + 2\alpha P_i < 0 \\ &\begin{bmatrix} -rP_i & \overline{A}_i^{kg} P_i \\ \overline{A}_i^{kg} P_i & -rP_i \end{bmatrix} < 0 \\ &\begin{bmatrix} \sin\theta \left(\overline{A}_i^{kg} P_i + P_i \left(\overline{A}_i^{kg}\right)^T\right) & \cos\theta \left(\overline{A}_i^{kg} P_i - P_i \left(\overline{A}_i^{kg}\right)^T\right) \\ \cos\theta \left(P_i \left(\overline{A}_i^{kg}\right)^T - \overline{A}_i^{kg} P_i\right) & \sin\theta \left(\overline{A}_i^{kg} P_i + P_i \left(\overline{A}_i^{kg}\right)^T\right) \end{bmatrix} \\ &< 0. \end{aligned} \tag{60}$$

After solving the mixed H_2/H_∞ problem shown in (58)–(60), the attenuation level ρ^2 can be minimized so that the performance degradation due to $\overline{w}_i$ is minimized; that is,

$$\min_{P_i} \quad \rho^2 \qquad \text{Subject to} \quad (58)\text{–}(60). \tag{61}$$

It should be pointed out that (59) and (60) are not convex, which can not be directly solved by using LMI technology. Fortunately, by using the Schur complement, those inequalities can be transferred into three eigenvalue problems with constrain of LMIs [20], which is convex and can be solved easily by using Matlab LMI toolbox.

It is noted here that the stability of the closed-loop system in (21) can be guaranteed by (47) at the equilibrium $\overline{x}_i(t) = 0$ without considering the disturbance $\overline{w}_i$, of which proof is given in Appendix A.2.

Then, the mixed H_2/H_∞ problem shown in (58)–(60) can be solved by using LMI technology. However, it is difficult to give the appropriate values of those bounding matrixes shown in (23)–(29). This paper adopts an iteration processer to obtain the suitable values of bounding matrixes ΔA_i, ΔB_i, ΔC_i, ΔD_i, ΔE_i, ΔF_{xi}, and ΔF_{yi} [20].

Assumption Correction Processer

(a) Give an initial attenuation level ρ^2 and the bounding matrixes, select weighting matrixes Q_{1i}, Q_{2i}, and R_i, and solve the problem in (58) to obtain the observer gain L_i^k and the controller parameters k_{pi}^k and k_{ii}^k.

(b) Check assumption (23)–(29). If they are not satisfied, expand the bounds for all elements in ΔA_i, ΔB_i, ΔC_i, ΔD_i, ΔE_i, ΔF_{xi}, and ΔF_{yi}, and then repeat (a)-(b).

(c) Check positive definiteness of ${P_{i11}}^{-1} > 0$, $P_{i22} > 0$, and ${P_{i33}}^{-1} > 0$ (where $P_i = blk\,\mathrm{diag}\{P_{i11}, P_{i22}, P_{i33}\}$). If it is not satisfied, increase ρ and then repeat (b)-(c).

(d) Substitute P_i and ρ into (59) and (60) to confirm the stability and verify those inequalities.

When the appropriate values of the bounding matrixes have been obtained, the neural adaptive observer in (12) and mixed H_2/H_∞ neural PI controller in (18) can be constructed. It is noted that in the second step of the above iteration method, (26)-(27) involves global variables E_j' and δ_{ij}. Before constructing the observer and the controller, the correction of ΔD_i and ΔE_i should be solved in a decentralized approach.

From (10) and (11), we get

$$\begin{aligned} \Delta d_{xi} &\le d_{xi}\left(\left|E_j'\right|_{\max}, 1\right) - \sum_{k=1}^{n} \mu_k \left(I_{mxi}^k + T_{wi}^k\right) \le \Delta D_i x_i \\ \Delta d_{yi} &\le d_{yi}\left(\left|E_j'\right|_{\max}, 1\right) - \sum_{k=1}^{n} \mu_k I_{myi}^k \le \Delta E_i x_i. \end{aligned} \tag{62}$$

$|E_j'|_{\max}$ is the prescribed value according the normal capacity of the jth generator, and T_{wi}, I_{mxi}, and I_{myi} can be computed by only using local signals. Thus, the correction of ΔD_i and ΔE_i of (26) and (27) can be replaced by (62), where the decentralized control is achieved.

From the above derivations, it is seen that the neural weighting controller is proposed to cope with the nonlinearity of DFIG, and approximation error caused by neural approximation and parameter uncertainty has been considered and stabilized by a proposed robust controller. Based on the characteristics of power system, several advanced technologies have been integrated smoothly into the proposed

Table 1: Parameter of DFIG (per unit: $S_{base} = 10$ WM; $V_{base} = 575$ V).

Parameter	R_s	L_s	R_r	L_r	L_m	H_{tot}	Converter capacity
Value in pu	0.007	0.171	0.005	0.156	2.9	5.04	50%

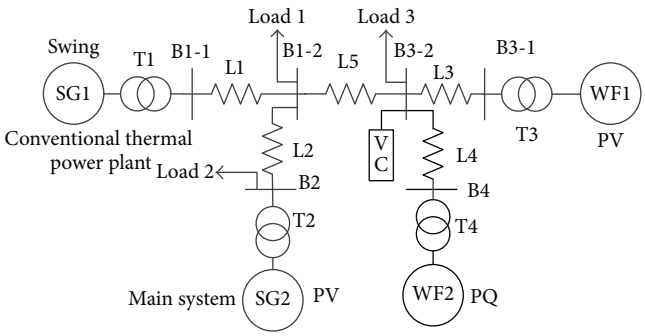

Figure 3: Multimachine power system model for assessing the performance of the proposed controller.

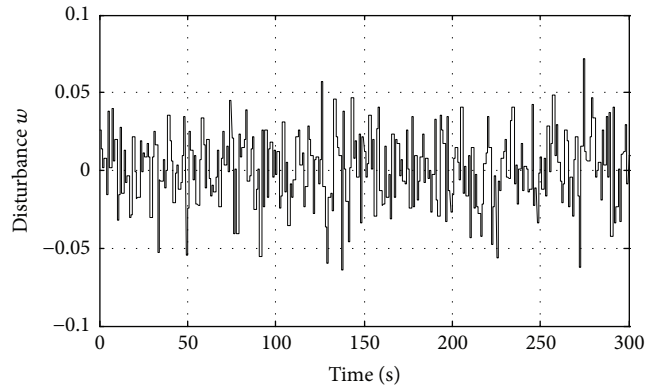

Figure 4: Stochastic disturbance $\overline{w}_i$.

neural PI controller, which leads to a multiobjective optimization in comparison with the conventional PI controller which is a signal-objective control.

It is seen that the proposed neural PI controller has a similar structure as the conventional PI controller, which takes the natural advantage of conventional PI controller in tracking control. However, the proposed neural PI controller considers the interactions from network which is represented by only using local variables. This means system-wide feedback control can be replaced by only using local variables. Thus, the proposed controller can be regarded as a decentralized coordinated control, which is a desired result for the controller design of large-scale geographically extensive systems.

4. Simulations

For assessing the performance of the proposed controller, a multimachine power system shown in Figure 3 is modelled in Matlab/Simulink, and the parameters of DFIG are given in Tables 1 and 2. The power system model consists of two fields, the load center comprised by two SGs, and the remote terminal comprised of two DFIG-based WFs. Those two fields are connected by the transmission line L5 with a long distance of 200 km to investigate the proposed controller capabilities in a weak power system, which is difficult to guarantee the LVRT capability of DFIG, especially under sensor fault case. In order to restore the terminal voltage of WFs, a Var compensator (VC) is connected to the common coupling point (CCP) of WFs Bus B3-2.

In this section, the capabilities of the proposed control strategy are assessed under small disturbance and large disturbance, respectively. The small disturbance is identified as a slight sensor fault, which is mimicked by a bounded stochastic disturbance shown in Figure 4. The large disturbance is the slight sensor fault plus three-phase ground faults. For comparison purpose, the responses with the conventional PI (CPI) controller is also presented and discussed. In order to simplify the introduction, the proposed control strategy is identified as the neural PI (NPI) controller.

4.1. Responses to Small Disturbances. In this subsection, a slight sensor fault represented by a stochastic bounded disturbance shown in Figure 4 is applied in the sensor of active power. The WF1 responses with the proposed neural PI controller and the conventional PI controller are shown in Figure 5.

It can be seen that the MPPT performance with the CPI controller is reduced drastically under the disturbance $\overline{w}_i$. (P_e of Figure 5(b)), which causes the dc-link voltage v_{dc} oscillated seriously (v_{dc} of Figure 5(b)). However, the MPPT performance under the same sensor fault is still acceptable when the NPI controller is installed. It can be seen that the effect of the disturbance $\overline{w}_i$ has been efficiently suppressed by the H_∞ controller, and the oscillation bound of P_e with the NPI controller is narrow (P_e of Figure 5(a)), which helps to smooth the dc-link voltage (v_{dc} of Figure 5(a)). It can be seen that the oscillation of v_{dc} is very small when the NPI controller is used.

In order to show this difference directly, the integral of absolute error (IAE) defined as IAE $= \int_{t_0}^{t_f} |P_{eref} - P_e| dt$ is used to evaluate the MPPT performances with different controllers. The IAE is 251 when the NPI controller is used. However, the value with the CPI controller is 526, which is two times of that with the NPI controller.

It is concluded that the MPPT performance under the slight sensor fault has been considerably improved by the NPI controller, which is valuable for WFs installed in the remote regions without timely maintenance.

4.2. Responses to Large Disturbances. In this subsection, a three-phase ground fault is applied in the middle of line L1 at $t = 0+$, and it is cleared after 0.1 s. The responses of WF1 with the NPI and CPI controllers are shown in Figure 6(a).

Table 2: Parameter of the conventional PI controller [14].

Parameter	Power regulator	Voltage regulator	Rotor current regulators
Proportion coefficient	$k_{pp} = 1$	$k_{vp} = 1.25$	$k_{idp} = k_{iqp} = 0.3$
Integration coefficient	$k_{pi} = 100$	$k_{vi} = 300$	$k_{idi} = k_{iqi} = 7$

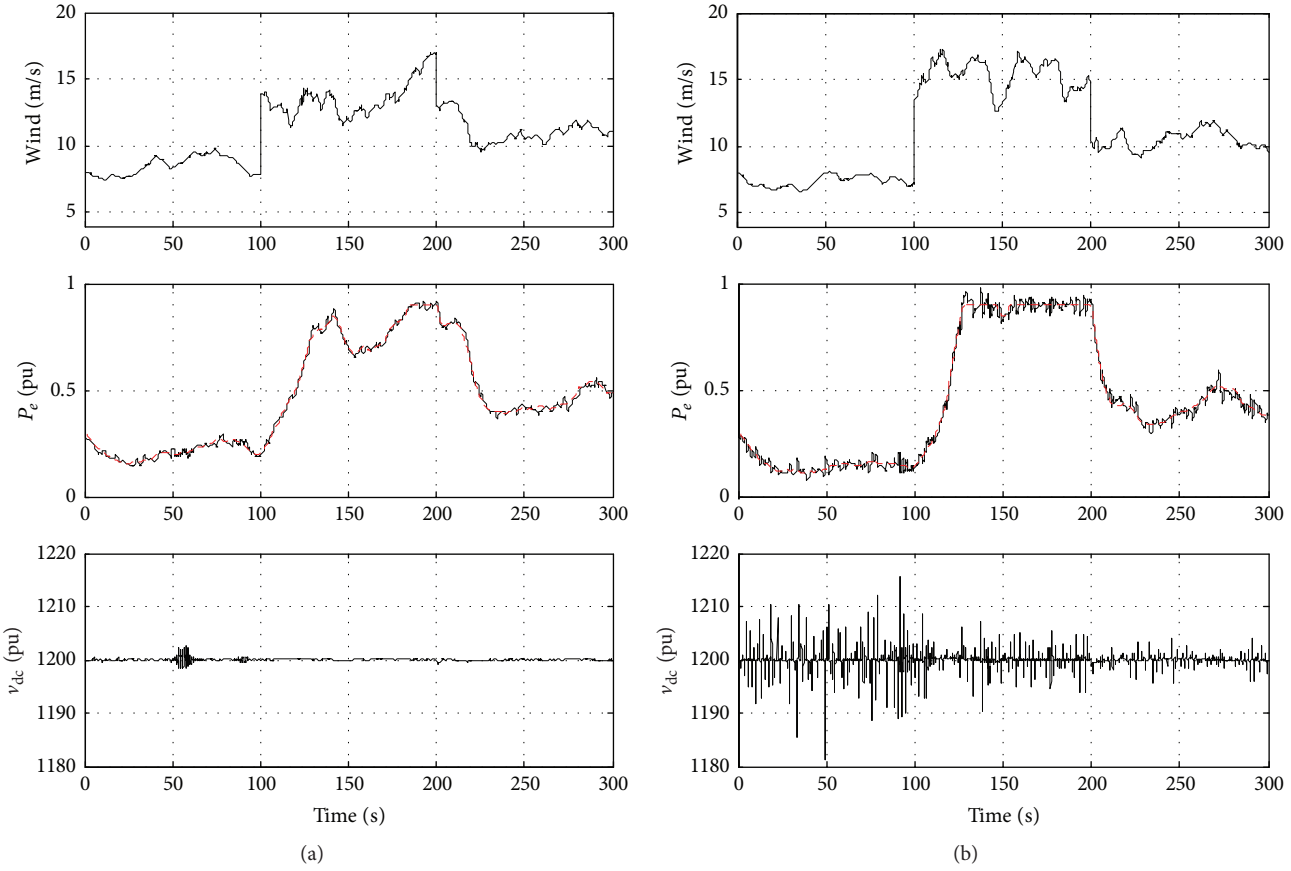

Figure 5: MPPT performances with sensor fault: (a) NPI controller; (b) CPI controller.

For illustrating the contribution to network supports, the response of Bus B1-2 which is the CCP of SGs is also presented in Figure 6(b).

It is seen that both the NPI controller and CPI controller can provide acceptable damping performance; however the NPI controller is better (P_e of Figure 6(a)). Since the NPI controller has achieved an effective control of internal voltage vector by reducing its angle jump, the terminal voltage drop is smaller in comparison with the CPI controller used. The smaller terminal voltage drop makes DFIG output more active power in the faults. Thus, less active power is accumulated in the dc-link, which reduces the peak value of dc-link voltage (v_{dc} of Figure 6(a)). Terminal under voltage and dc-link over voltage are regarded as two major reasons to limit LVRT capability of DFIG, which have been considerably improved by the NPI controller.

Figure 6(b) shows the contribution of the NPI controller to network supports, such as improved system damping (P_e of Figure 6(b)), better terminal voltage recovery capability ($|v_s|$ of Figure 6(b)), and system frequency support (Hz of Figure 6(b)).

4.3. Contribution on Transient Stability. A three-phase ground fault is applied in the terminal of transformer T3 at $t = 0+$, and it is cleared after 0.1 s. The fault is closer to the WF1, which means that the disturbance is more serious. The system responses are shown in Figure 7.

It is seen that, under such a large disturbance, the WF1 with the CPI controller is tripped at $t = 0.1084$ s for terminal under voltage ($|v_s|$ of Figure 7(a)) and its output active power drops to zero at the same time (P_e of Figure 7(a)). The trip of WF1 leads to surplus reactive power, which rises the terminal voltage of WF2 and triggers the terminal over voltage protection to trip the WF2 at $t = 0.2481$ (P_e of Figure 7(b)). The trip of WFs makes power system lose large-scale active power in a very short time. Since the large inertial of thermal power plant, the SGs are not capable of generating the corresponding active power immediately, which drops the rotor speed of

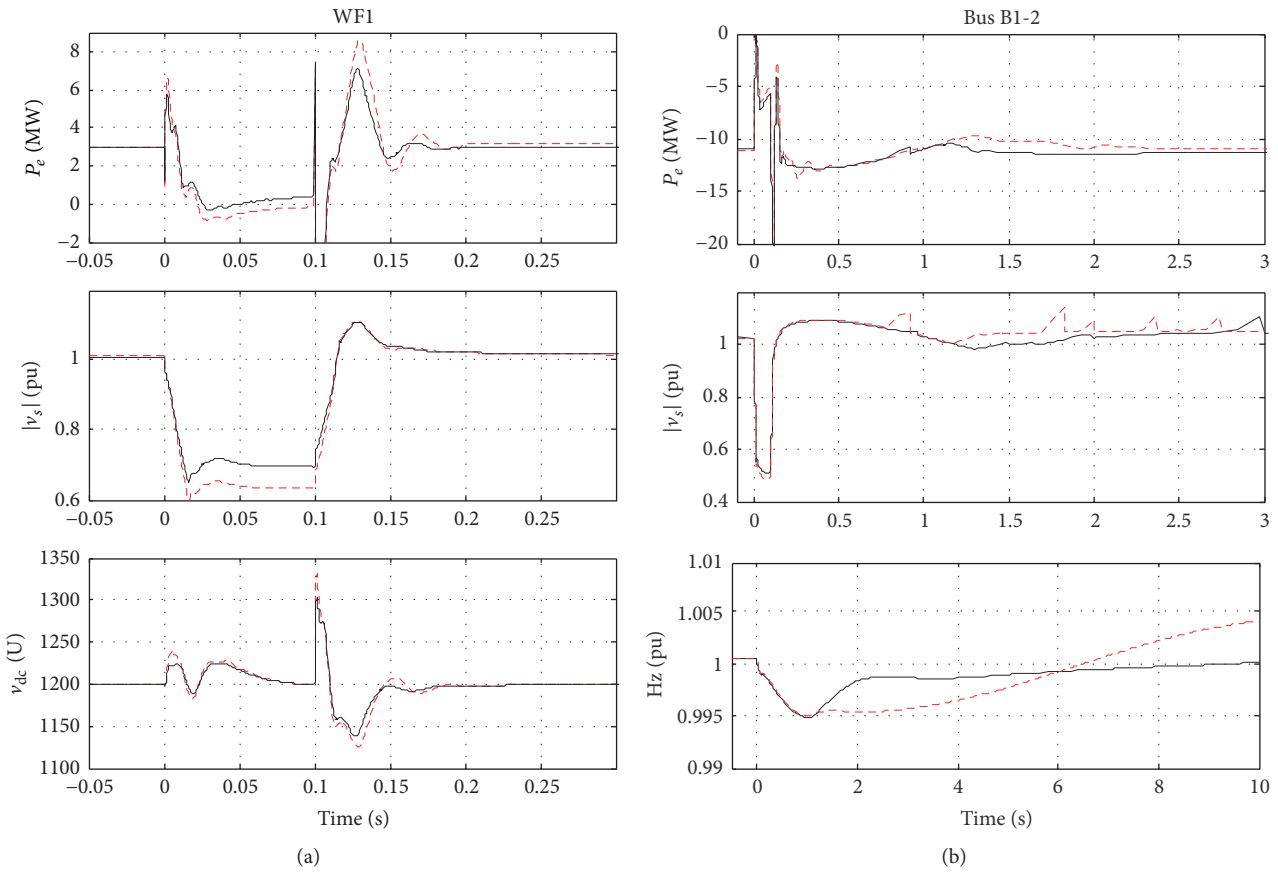

Figure 6: Fault responses at $s_1 = 0.2$ pu: NPI controller (full line); CPI controller (dashed line).

Table 3: Operating points chosen for establishing the model bank (motor convention).

Operating point	u_{ds}	u_{qs}	i_{ds}	i_{qs}	v_{dr}	v_{qr}	P_e	Q_e
$\omega_r = 0.80$	−1.0	0.0	0.3	0.34	−0.32	−0.03	−0.2	0.36
$\omega_r = 0.92$	0.1	−1.0	−0.4	0.4	0.03	−0.1	−0.4	0.36
$\omega_r = 0.97$	−0.39	0.93	0.51	−0.3	−0.02	0.03	−0.46	0.36
$\omega_r = 1.03$	1.0	−0.14	−0.64	−0.28	−0.04	−0.003	−0.62	0.37
$\omega_r = 1.12$	−1.0	−0.19	0.57	0.48	0.09	0.04	−0.71	0.37
$\omega_r = 1.20$	−0.45	0.9	0.65	−0.49	0.13	−0.15	−0.89	0.36

SG1 ω_r from 1 pu to 0.9954 pu (ω_r of Figure 7(c)) very quickly. This may cause the SG1 to be tripped and leads to imbalance of active power, which leads to frequency collapse and further worsens power system transient stability.

It is seen that, as opposed to the CPI controller, the NPI controller ensures that WF1 can be connected to the grid with acceptable rotor speed (ω_r of Figure 7(a)), which provides DFIG with continuing network support capability to balance the active power and reactive power. Thus, the power system frequency can be operated in a permissible range. It is noticeable that the NPI controller provides the system with good terminal voltage recovery capability ($|v_s|$ of Figure 7).

Figures 6 and 7 show the capabilities of the NPI controller to improve system damping, MPPT, LVRT, and its contribution to network support at both subsynchronous and supper synchronous conditions.

5. Conclusions

This paper proposes an adaptive neural decentralized coordinated control of DFIG, where a neural interaction measurement observer is proposed to approximate the nonlinear model of DFIG. The approximation error due to neural approximation has been considered, and a robust stabilization technique is also proposed to override the effect of the approximation error. For considering the slight sensor fault represented by stochastic disturbance, the H_∞ controller is employed to suppress the fault effect. The H_2 controller is also employed to achieve specified engineering purposes. Then, the proposed controller can be formulated as a mixed H_2/H_∞ optimization problem with constrains of PI structure and regional pole placement, which can be solved by using LMI technique. Simulation results are presented and discussed,

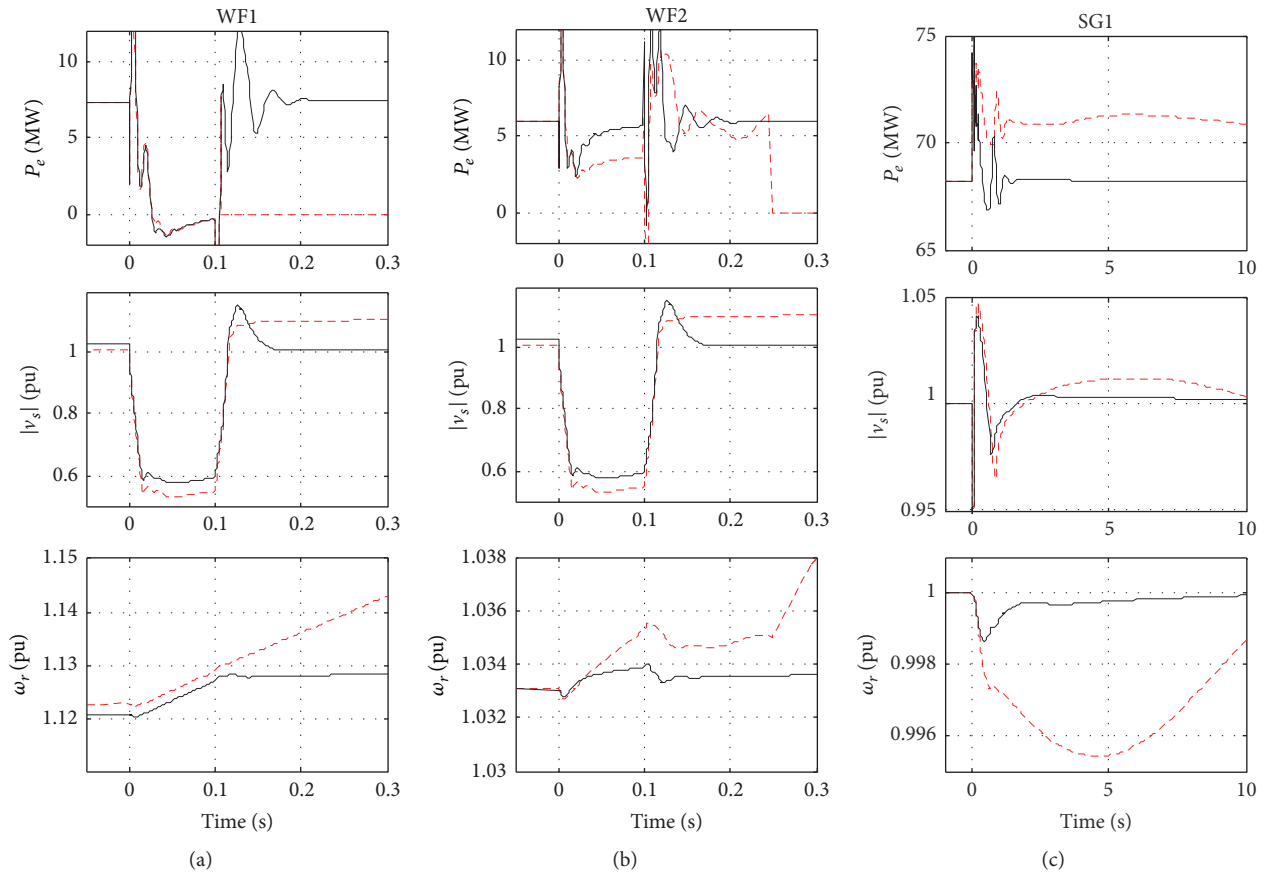

FIGURE 7: Fault responses at $s_1 = -0.122$ pu: NPI controller (full line); CPI controller (dashed line).

which demonstrate the capabilities of the proposed control strategy to system damping, voltage recovery and LVRT, and its contributions on power system transient stability, especially for frequency support.

This paper demonstrates that, in comparison with the conventional PI controller, the proposed control strategy provides DFIG with the greater capabilities of fault-tolerant control of MPPT and continuing network support during power system fault conditions.

Appendix

A. Proofs of the Upper Bound and the Stability

A.1. Upper Bound Computation. For a DFIG-based wind turbine, the reference value of output active power P_{eref} is determined by the mechanical torque of wind turbine, which is written as following form [21]:

$$T_{mi} = \left(\frac{0.5\rho_{\text{air}} S_{wt} R_{wt} C_{P\text{-max}}}{\lambda_{\text{opt}}} \right)_i \omega_{wti}^2 = K'_{wti} \omega_{ri}^2. \tag{A.1}$$

By linearizing (A.1), we have

$$\Delta T_{mi}^k = 2K'_{wti} \omega_{ri0} \Delta\omega_{ri} = \left[2\omega_{ri0} K'_{wti} \quad 0 \quad 0 \right] x_i. \tag{A.2}$$

The maximum rotor speed ω_{ri} is 1.2 pu; then the following inequality can be obtained:

$$\left\| \sum_{k=1}^{n} \mu_k T_{wi}^k \right\|_2 \le \left\| \left[2.4K'_{wti} \quad 0 \quad 0 \right] x_i \right\|_2 = \left\| \Delta H_i x_i \right\|_2. \tag{A.3}$$

It is known that the maximum reference values of output active power and reactive power of DFIG are determined by its mechanical power $P_{mi} = T_{mi}\omega_{wti}$ and apparent power S_i.

$$\begin{aligned} P_{\text{eref}i} &\le K'_{wti} \omega_{ri}^3 \\ Q_{\text{eref}i} &\le |S_i| \le \left| \vec{E}'_i \right| \max\left(\left| \vec{i}^{\,*}_{si} \right| \right) < \sqrt{E'^2_{di} + E'^2_{qi}}, \end{aligned} \tag{A.4}$$

where the maximum value of $|\vec{i}^{\,*}_{si}|$ is the normal capacity of DFIG, of which value is less than 1 pu.

By linearizing (A.4), we have

$$\begin{aligned} \Delta P_{\text{eref}i} &\le 3K'_{wti} \omega_{ri0}^2 \Delta\omega_{ri} = \left[3K'_{wti} \omega_{ri0}^2 \quad 0 \quad 0 \right] x_i \\ \Delta Q_{\text{eref}i} &< \frac{E'_{di0}}{|E'_i|_0} \Delta E'_{di} + \frac{E'_{qi0}}{|E'_i|_0} \Delta E'_{qi} \\ &= \begin{bmatrix} 0 & \dfrac{E'_{qi0}}{|E'_i|_0} & \dfrac{E'_{di0}}{|E'_i|_0} \end{bmatrix} x_i. \end{aligned} \tag{A.5}$$

Then, we obtain

$$\left\|r_i\right\|_2 \le \left\|\Delta G_i x_i\right\|_2. \tag{A.6}$$

A.2. Stability Proof. Before solving the mixed H_2/H_∞ suboptimization problem, the stability of the closed-loop system in (21) should be guaranteed at the equilibrium $\overline{x}_i(t) = 0$ without considering the disturbance $\overline{w}_i$. The Lyapunov function of system of (21) is chosen as

$$\begin{aligned}\dot{V} &= \dot{\overline{x}}_i^T P_{i1}\overline{x}_i + \overline{x}_i^T P_{i1}\dot{\overline{x}} \\ &= \left(\sum_{k=1}^{n}\mu_k\sum_{g=1}^{n}\mu_g\overline{A}_i^{kg}\overline{x}_i\right)^T P_{1i}\overline{x}_i \\ &\quad + \overline{x}_i^T P_{1i}\left(\sum_{k=1}^{n}\mu_k\sum_{g=1}^{n}\mu_g\overline{A}_i^{kg}\overline{x}_i\right) + \Delta f_{gh}^T P_{1i}\overline{x}_i \\ &\quad + \overline{x}_i^T P_{1i}\Delta f_{gh}.\end{aligned} \tag{A.7}$$

From (45), (A.7) can be rewritten as

$$\begin{aligned}\dot{V} = \dot{\overline{x}}_i^T P_{i1}\overline{x}_i + \overline{x}_i^T P_{i1}\dot{\overline{x}} &\le \left(\sum_{k=1}^{n}\mu_k\sum_{g=1}^{n}\mu_g\overline{A}_i^{kg}\overline{x}_i\right)^T P_{1i}\overline{x}_i \\ &\quad + \overline{x}_i^T P_{1i}\left(\sum_{k=1}^{n}\mu_k\sum_{g=1}^{n}\mu_g\overline{A}_i^{kg}\overline{x}_i\right) + \left(\varphi_{fi}\overline{x}_i\right)^T\left(\varphi_{fi}\overline{x}_i\right) \\ &\quad + \sum_{k=1}^{n}\mu_k\left\{\left(\varphi_{gi}^k\overline{x}_i\right)^T\left(\varphi_{gi}^k\overline{x}_i\right)\right\} + 2\sum_{k=1}^{n}\mu_k \\ &\quad \cdot\left\{\left(\varphi_{h1i}^k\overline{x}_{ii}\right)^T\left(\varphi_{h1i}^k\overline{x}_{ii}\right)\right\} + \left(\varphi_{h2i}\overline{x}_i\right)^T\left(\varphi_{h2i}\overline{x}_i\right) \\ &\quad + \left(\varphi_{ri}\overline{x}_i\right)^T\left(\varphi_{ri}\overline{x}_i\right) + \left(\varphi_{dxi}\overline{x}_i\right)^T\left(\varphi_{dxi}\overline{x}_i\right) + 2\sum_{k=1}^{n}\mu_k \\ &\quad \cdot\left\{\left(\varphi_{dy1i}^k\overline{x}_i\right)^T\left(\varphi_{dy1i}^k\overline{x}_i\right)\right\} + \left(\varphi_{dy2i}\overline{x}_i\right)^T\left(\varphi_{dy2i}\overline{x}_i\right) \\ &\quad + \left(\varphi_{di}\overline{x}_i\right)^T\left(\varphi_{di}\overline{x}_i\right) + \sum_{k=1}^{n}\mu_k\left\{\left(\varphi_{mxi}^k\overline{x}_i\right)^T\left(\varphi_{mxi}^k\overline{x}_i\right)\right. \\ &\quad \left.+ \left(\varphi_{myi}^k\overline{x}_i\right)^T\left(\varphi_{myi}^k\overline{x}_i\right)\right\} + 8\overline{x}_i^T P_{1i}P_{1i}\overline{x}_i = \sum_{k=1}^{n}\mu_k \\ &\quad \cdot\sum_{g=1}^{n}\mu_g\overline{x}_i^T\left(\left(\overline{A}_i^{kg}\right)^T P_{1i} + P_{1i}\left(\overline{A}_i^{kg}\right) + \left(\varphi_{fi}\right)^T\left(\varphi_{fi}\right)\right. \\ &\quad + 2\left(\varphi_{gi}^k\right)^T\left(\varphi_{gi}^k\right) + 2\left(\varphi_{h1i}^k\right)^T\left(\varphi_{h1i}^k\right) + \left(\varphi_{h2i}^k\right)^T \\ &\quad \cdot\left(\varphi_{h2i}^k\right) + \left(\varphi_{ri}\right)^T\left(\varphi_{ri}\right) + \left(\varphi_{dxi}\right)^T\left(\varphi_{dxi}\right) + \left(\varphi_{dy1i}^k\right)^T \\ &\quad \cdot\left(\varphi_{dy1i}^k\right) + \left(\varphi_{dy2i}\right)^T\left(\varphi_{dy2i}\right) + \left(\varphi_{di}\right)^T\left(\varphi_{di}\right) \\ &\quad \left.+ \left(\varphi_{mxi}^k\right)^T\left(\varphi_{mxi}^k\right) + \left(\varphi_{myi}^k\right)^T\left(\varphi_{myi}^k\right) + 8P_{1i}P_{1i}\right)\overline{x}_i.\end{aligned} \tag{A.8}$$

According (47), (A.8) can be rewritten as

$$\begin{aligned}\dot{V} = \dot{\overline{x}}_i^T P_{i1}\overline{x}_i + \overline{x}_i^T P_{i1}\dot{\overline{x}} &\le \sum_{k=1}^{n}\mu_k\sum_{g=1}^{n}\mu_g \\ &\quad \cdot\overline{x}_i^T\left[-\rho^{-2}P_{1i}\left(\overline{E}_i^{\,k}\left(\overline{E}_i^{\,k}\right)^T + 8I\right)P_{1i} - Q_{1i}\right]\overline{x}_i \\ &\quad < 0.\end{aligned} \tag{A.9}$$

It is seen the closed-loop system of (21) is locally quadratically stable at the equilibrium $\overline{x}_i(t) = 0$ without considering the disturbances $\overline{w}_i$.

Nomenclature

v_s, v_r:	Stator and rotor voltages
i_s, i_r:	Stator and rotor currents
E':	Internal voltage
P_e, Q_e:	Output active power and reactive power of DFIG
P_s, Q_s:	Output active power and reactive power of stator of DFIG
T_m, T_e:	Mechanical torque and electric torque of DFIG
R_s, R_r:	Stator and rotor resistances
X_s', X_s:	Transient and open-circuit reactances
L_{ss}, L_{rr}:	Stator and rotor self-inductances
L_m:	Mutual inductance
T_0':	Transient open-circuit time constant
δ_{12}:	Power angle difference between SG1 and SG2
s, ω_r:	Rotor slip and rotor speed
d, q:	Subscript for component of d and q axis
x, y:	Subscript for component of x and y-axis
ref:	Subscript for reference value.

Conflicts of Interest

The authors declare that there are no conflicts of interest regarding the publication of this paper.

Acknowledgments

This work is supported by the National Key Basic Research Program of China (973 Program) under Grant no. 2012CB215203, by the National Nature Science Foundation of China under Grant nos. 51606033, 61673101, 61203043, and 61304015, and by the Major Project of Jilin Science and Technology Development Program under Grant no. 20150203001SF.

References

[1] D. Gautam, V. Vittal, and T. Harbour, "Impact of increased penetration of DFIG-based wind turbine generators on transient and small signal stability of power systems," *IEEE Transactions on Power Systems*, vol. 24, no. 3, pp. 1426–1434, 2009.

[2] A. D. Hansen and G. Michalke, "Fault ride-through capability of DFIG wind turbines," *Renewable Energy*, vol. 32, no. 9, pp. 1594–1610, 2007.

[3] A. Morattab and O. Akhrif, "Decentralized coordinated secondary voltage control of multi-area power grids using model predictive control," *IET Generation, Transmission and Distribution*, 2017.

[4] S. Shukla and L. Mili, "Hierarchical decentralized control for enhanced rotor angle and voltage stability of large-scale power systems," *IEEE Transactions on Power Systems*, 2017.

[5] F. Rezaei and S. Esmaeili, "Decentralized reactive power control of distributed PV and wind power generation units using an optimized fuzzy-based method," *International Journal of Electrical Power and Energy Systems*, vol. 87, pp. 27–42, 2017.

[6] C.-L. Chen and Y.-Y. Hsu, "Coordinated synthesis of multimachine power system stabilizer using an efficient decentralized modal control (DMC) algorithm," *IEEE Transactions on Power Systems*, vol. 2, no. 3, pp. 543–550, 1987.

[7] F. F. Wu, K. Moslehi, and A. Bose, "Power system control centers: Past, present, and future," *Proceedings of the IEEE*, vol. 93, no. 11, pp. 1890–1908, 2005.

[8] C.-X. Dou, J. Yang, X. Li, T. Gui, and Y. Bi, "Decentralized coordinated control for large power system based on transient stability assessment," *International Journal of Electrical Power and Energy Systems*, vol. 46, no. 1, pp. 153–162, 2013.

[9] A. M. Fombu, G. Kenné, J. D. D. Nguimfack-Ndongmo, and R. Kuate-Fochie, "Decentralized nonlinear coordinated excitation and steam valve adaptive control for multi-machine power systems," *International Journal of Electrical Power and Energy Systems*, vol. 75, pp. 117–126, 2016.

[10] C.-X. Dou, D.-W. Hao, B. Jin, W.-Q. Wang, and N. An, "Multiagent-system-based decentralized coordinated control for large power systems," *International Journal of Electrical Power and Energy Systems*, vol. 58, pp. 130–139, 2014.

[11] Q. Sun, R. Han, H. Zhang, J. Zhou, and J. M. Guerrero, "A Multiagent-Based Consensus Algorithm for Distributed Coordinated Control of Distributed Generators in the Energy Internet," *IEEE Transactions on Smart Grid*, vol. 6, no. 6, pp. 3006–3019, 2015.

[12] M. G. Singh, *Decentralized Control*, Elsevier Science Inc, Georgia, Ga, USA, 1981.

[13] D. D. Sijjak, *Decentralized Control of Complex Systems*, Courier Corporation, Massachusetts, Mass, USA, 2011.

[14] R. Pena, J. C. Clare, and G. M. Asher, "Doubly fed induction generator using back-to-back PWM converters and its application to variablespeed wind-energy generation," *IEE Proceedings-Electric Power Applications*, vol. 143, no. 3, pp. 231–241, 1996.

[15] J. B. Ekanayake, L. Holdsworth, and N. Jenkins, "Comparison of 5th order and 3rd order machine models for doubly fed induction generator (DFIG) wind turbines," *Electric Power Systems Research*, vol. 67, no. 3, pp. 207–215, 2003.

[16] Y.-G. Niu, X.-M. Li, Z.-W. Lin, and M.-Y. Li, "Multiple models decentralized coordinated control of doubly fed induction generator," *International Journal of Electrical Power and Energy Systems*, vol. 64, pp. 921–930, 2015.

[17] Y. Niu, X. Li, and Z. Lin, "Decentralized coordinated neural control of doubly fed induction generator based wind farm for power system stability support," *Journal of Renewable and Sustainable Energy*, vol. 6, no. 4, Article ID 043126, 2014.

[18] F.-J. Lin, K.-H. Tan, and C.-H. Tsai, "Improved differential evolution-based Elman neural network controller for squirrel-cage induction generator system," *IET Renewable Power Generation*, vol. 10, no. 7, pp. 988–1001, 2016.

[19] M. Chilali and P. Gahinet, "H_∞ design with pole placement constraints: an LMI approach," *IEEE Transactions on Automatic Control*, vol. 41, no. 3, pp. 358–367, 1996.

[20] B.-S. Chen, C.-S. Tseng, and H.-J. Uang, "Mixed H_2/H_∞ fuzzy output feedback control design for nonlinear dynamic systems: An LMI approach," *IEEE Transactions on Fuzzy Systems*, vol. 8, no. 3, pp. 249–265, 2000.

[21] O. Anaya-Lara, N. Jenkins, J. Ekanayake et al., *Wind Energy Generation: Modelling and Control*, John Wiley and Sons, New Jersey, NJ, USA, 2011.